

**Numerical integration
of troposphere
photochemistry
mechanism**

F. Liu et al.

Technical note: application of α -QSS to the numerical integration of kinetic equations in tropospheric chemistry

F. Liu¹, E. Schaller¹, and D. R. Mott²

¹Department of Environmental Meteorology, BTU Cottbus, Germany

²Laboratory for Computational Physics and Fluid Dynamics, Naval Research Laboratory, Washington, DC 20375-5320, USA

Received: 9 May 2005 – Accepted: 6 July 2005 – Published: 18 August 2005

Correspondence to: F. Liu (lfeng@tu-cottbus.de)

© 2005 Author(s). This work is licensed under a Creative Commons License.

Title Page

Abstract

Introduction

Conclusions

References

Tables

Figures

⏪

⏩

◀

▶

Back

Close

Full Screen / Esc

Print Version

Interactive Discussion

Abstract

A major task in many applications of atmospheric chemistry transport problems is the numerical integration of stiff systems of Ordinary Differential Equations (ODEs) describing the chemical transformations. A faster solver that is easier to couple to the other physics in the problem is still needed. The integration method, α -QSS, corresponding to the solver CHEMEQ2 aims at meeting the demands of a process-split, reacting-flow simulation (Mott 2000; Mott and Oran, 2001). However, this integrator has yet to be applied to the numerical integration of kinetic equations in tropospheric chemistry. A zero-dimensional (box) model is developed to test how well CHEMEQ2 works on the tropospheric chemistry equations. This paper presents the testing results. The reference chemical mechanisms herein used are Regional Atmospheric Chemistry Mechanism (RACM) (Stockwell et al., 1997) and its secondary lumped successor Regional Lumped Atmospheric Chemical Scheme (ReLACS) (Crassier et al., 2000). The box model is forced and initialized by the DRY scenarios of Protocol Ver.2 developed by EUROTRAC (Poppe et al., 2001). The accuracy of CHEMEQ2 is evaluated by comparing the results to solutions obtained with VODE. This comparison is made with parameters of the error tolerance, relative difference with respect to VODE scheme, trade off between accuracy and efficiency, global time step for integration etc. The study based on the comparison concludes that the single-point α -QSS approach is fast and moderately accurate as well as easy to couple to reacting flow simulation models, which makes CHEMEQ2 one of the best candidates for three-dimensional atmospheric Chemistry Transport Modelling (CTM) studies. In addition the RACM mechanism may be replaced by ReLACS mechanism for tropospheric chemistry transport modelling. The testing results also imply that the accuracy for chemistry numerical simulations is highly different from species to species. Therefore ozone is not the good choice for testing numerical ODE solvers or for evaluation of mechanisms because current tropospheric chemistry mechanisms are mainly designed for troposphere ozone prediction.

Numerical integration of troposphere photochemistry mechanism

F. Liu et al.

Title Page

Abstract

Introduction

Conclusions

References

Tables

Figures

⏪

⏩

◀

▶

Back

Close

Full Screen / Esc

Print Version

Interactive Discussion

1. Introduction

For the improvement of understanding the transport and fate of trace gases and pollutants in the atmosphere, comprehensive atmospheric Chemistry and Transport Models (CTMs) have been developed. The operator splitting approach is very often used in the numerical solution of these equations. A major task is then the numerical integration of the stiff Ordinary Differential Equation (ODE) system describing the chemical transformation in the atmosphere, which leads to two important aspects that must be considered: efficiency and accuracy. Efficiency requires a relatively fast chemical solver. Because the corresponding ODEs are stiff, their solution normally requires at least 50% of the total CPU time. In studies on chemical integrations alone and in the development of atmospheric chemistry mechanisms, some standard stiff ODEs solvers have been intensively used, and they continue to be refined and developed (Gear, 1971; Hindmarsh, 1983; Hindmarsh and Norsett, 1988; Brown et al., 1989; Hairer and Wanner, 1991; Radhakrishnan and Hindmarsh, 1993). These solvers designed for chemistry stand-alone solutions of ODEs are very accurate but computationally more expensive per time step due to the use of the solution from several previous time steps.

In a CTM chemical transformations are only one of several processes, including in addition transport, turbulent diffusion, wet scavenging etc. The total change of the concentration of species i , n_i , can be derived from the mass conservative principle, i.e.

$$\frac{\partial n_i}{\partial t} = -\frac{\partial}{\partial x_k} (n_i v_k) + \frac{\partial}{\partial x_k} \left(-\overline{n'_i v'_k} \right) + E_i - S_i + (P_i - L_i n_i) \quad (1)$$

using the operator (process) splitting approach. The basic idea of operator splitting is to calculate the effects of each individual process separately for a chosen global time step Δt_g , and then combine the results according to Eq. (1). The integration of the ODEs representing the chemical transformation during Δt_g , is a local initial value problem at each grid point. The ODE integrator may subdivide Δt_g into smaller steps Δt , referred to as the chemical time step, in order to obtain an accurate and stable solution. The Δt

Numerical integration of troposphere photochemistry mechanism

F. Liu et al.

Title Page

Abstract

Introduction

Conclusions

References

Tables

Figures

◀

▶

◀

▶

Back

Close

Full Screen / Esc

Print Version

Interactive Discussion

**Numerical integration
of troposphere
photochemistry
mechanism**

F. Liu et al.

[Title Page](#)[Abstract](#)[Introduction](#)[Conclusions](#)[References](#)[Tables](#)[Figures](#)[⏪](#)[⏩](#)[◀](#)[▶](#)[Back](#)[Close](#)[Full Screen / Esc](#)[Print Version](#)[Interactive Discussion](#)

is heavily dependent on the timescale of the chemistry system, and varies generally during the course of a simulation.

A faster and easier-coupling ODE integrator is one of the most important parts in a three dimensional CTM because the high demand of CPU time for chemical integration. Easier-coupling means that the integrator works well within the framework of a process-split reacting flow algorithm. For this purpose much faster but moderately accurate methods which are generally different from those designed for chemistry stand-alone solutions of ODE systems have been developed. The trade-offs between accuracy and efficiency must be considered for specific problems which have different requirements of accuracy (Young and Boris, 1977; Oran and Boris, 1987, 2000). Such faster algorithms are in use in atmospheric models. Comparisons between different solvers have been performed (Shieh et al, 1988; Hertel et al., 1993; Saylor and Ford, 1995; Verwer and Loon, 1995; Sandu et al., 1995, 1996; Lorenzini and Passoni, 1999). Some standard solvers show comparable efficiency and accuracy for different chemical schemes (Sandu et al., 1996). The accuracy level should be considered in relation to the global accuracy requirement of the CTM. Calculations of atmospheric dynamics are seldom more accurate than a few percent. Thus, any requirement to the chemical integrator to calculate the species concentrations more accurate than a few tenths of a percent is usually excessive. Therefore the chemical integrator may be of relatively low-order. Furthermore, since the integrator must solve multiple initial value problems, it is advantageous to use a single-point method that requires information only from the current time level to calculate the concentration at the end of each global time step.

As the first step to apply an efficient chemical integrator to a tropospheric CTM, a box model is developed and implemented. This paper presents the results of applying the ODE integration algorithm, α -QSS (Mott, et al., 2000; Mott and Oran, 2001), to tropospheric gas-phase chemistry within the box model. The solver CHEMEQ2 based on α -QSS was developed specifically to meet the above demands of a process-split, reacting-flow simulation.

This paper is organized as follows. Section 2 describes tropospheric chemistry

mechanisms and scenarios used for testing CHEMEQ2. In Sect. 3 we describe the α -QSS algorithm as implemented in CHEMEQ2. Section 4 includes testing results and Sect. 5 gives an analysis in respect to the accuracy and efficiency of the tested solver. The final Sect. 6 collects some general remarks and final conclusions.

2. Description of the applied chemical mechanisms RACM and ReLACS

Gas-phase reaction mechanisms consist of an inorganic and an organic parts, especially the inorganic chemistry in the atmosphere is well understood. The complexity lies in the representation of the organic part of the mechanism. Thousands of chemical reactions and products are found in the lower atmosphere. Explicit, highly detailed chemical mechanisms such as Master Chemical Mechanism (MCM) developed by Jenkin et al. (1997) and Derwent et al. (1998) attempt to treat all chemical species and reactions individually. However, the difficulties with explicit mechanisms are twofold. Firstly, it is difficult to identify the reactants, intermediates, products, and rate constants for reactions. Secondly, it is computationally complex for integrating the large number of equations. Therefore, most photochemical models use a lumped chemical mechanism or reduced mechanism, within which a surrogate species is created to present a group of individual organic species. The major approaches for lumping are either Lumped Structure (LS) or Lumped Molecule (LM) approach. Over the last few decades a series of lumped mechanisms and their successors have been proposed for the chemistry of the atmosphere, i.e. the Acid Deposition and Oxidant Mode II mechanism (ADOM-II) (Lurmann et al., 1986), the Carbon Bon Mechanism IV (CB-IV) (Gery et al., 1989), the Co-operative Programme for Monitoring and Evaluation of the Long-Range Transmission of Air Pollutants in Europe (EMEP) (Simpson et al., 1993, 1997), the second generation Regional Acid Deposition Model Mechanism (RADM2) (Stockwell et al., 1990), Euro-RADM (Stockwell and Kley, 1994), Regional Atmospheric Chemistry Mechanism (RACM) (Stockwell et al., 1997) and the Regional Lumped Atmospheric Chemical Scheme (ReLACS) (Crassier et al., 2000). Intercomparisons of some mechanisms

Numerical integration of troposphere photochemistry mechanism

F. Liu et al.

Title Page

Abstract

Introduction

Conclusions

References

Tables

Figures

◀

▶

◀

▶

Back

Close

Full Screen / Esc

Print Version

Interactive Discussion

**Numerical integration
of troposphere
photochemistry
mechanism**

F. Liu et al.

[Title Page](#)[Abstract](#)[Introduction](#)[Conclusions](#)[References](#)[Tables](#)[Figures](#)[⏪](#)[⏩](#)[◀](#)[▶](#)[Back](#)[Close](#)[Full Screen / Esc](#)[Print Version](#)[Interactive Discussion](#)

were carried out by Poppe et al. (1996), Kuhn et al. (1998), Stockwell et al. (1998), Jimenez et al. (2003) and Gross and Stockwell (2003). Since the publication of the earlier studies many chemistry data including rate constant and kinetic data have been revised and updated according to new laboratory work. The RACM mechanism is a substantially revised version of RADM2 mechanism from the more recent laboratory measurements. Thus, the RACM mechanism must be considered to be superior to the RADM2 mechanism although the RADM2 has been used in many CTMs to predict concentrations of oxidants and other air pollutants (Gross and Stockwell, 2003). The RACM mechanism was developed to simulate tropospheric chemistry from the surface to the upper troposphere in remote to polluted urban conditions. It includes 77 species and 237 reactions (see Appendix). Although the RACM mechanism is much smaller than MCM it is still too large and numerically expensive for long-term simulation in a CTM. As a simplified RACM the ReLACS is a relatively highly lumped mechanism. The ReLACS mechanism is derived from a new reactivity weighting approach and almost keeps all information in RACM (Crassier et al., 2000). The ReLACS reduces prognostic species and reactions from 67 and 237 in RACM to 37 and 128 (see Appendix). This paper aims at the evaluation of the fast solver CHEMEQ2 with RACM and lumped ReLACS mechanisms for use in a CTM.

3. Introduction to the α -QSS method

The concentration changes with time due to chemical reactions for a set of N chemical species are described by a system of N ordinary differential equations (ODEs),

$$\frac{dn_i}{dt} = P_i - L_i n_i \quad 1 \leq i \leq N \quad (2)$$

where i is the species index, n_i is the number density of i th species, and P_i and $L_i n_i$ are the production and loss terms, respectively. For tropospheric chemistry this ODE system is nonlinear, highly coupled, and very stiff. If P and L are constant, then Eq. (2)

Numerical integration of troposphere photochemistry mechanism

F. Liu et al.

Title Page

Abstract

Introduction

Conclusions

References

Tables

Figures

⏪

⏩

◀

▶

Back

Close

Full Screen / Esc

Print Version

Interactive Discussion

has an exact solution given by

$$n_i(t) = n_{i0}e^{(-t/\tau)} + P_i\tau \left(1 - e^{(-t/\tau)}\right) \quad (3)$$

where $\tau=1/L$ is the chemical time scale. Quasi-Steady-State (QSS) methods are based on the solution given by Eq. (3) (Verwer and van Loon, 1994; Verwer and Simpson, 1995; Jay et al., 1997; Radhakrishnan and Pratt, 1988). They differ in how they incorporate the time dependence of P_i and L_j . They must not be confused with “steady-state” methods, in which the net chemical source term for some species is assumed to be zero. In this work and in the literature cited above, QSS refers to using Eq. (3) as the starting point for deriving an ODE integrator that retains all the timescale information present in the chemical mechanism.

Next, we introduce a parameter α defined as

$$\alpha = \alpha(\Delta t/\tau) = \frac{1 - \tau/\Delta t \left(1 - e^{-\Delta t/\tau}\right)}{1 - e^{-\Delta t/\tau}} \quad (4)$$

and rearrange Eq. (3) to

$$n(\Delta t) = n_0 + \frac{\Delta t (P - n_0/\tau)}{1 + \alpha\Delta t/\tau} \quad (5)$$

The parameter α is a function of $\Delta t/\tau$, as shown in Fig. 1. The n/τ has to be non-negative, so only values of $\Delta t/\tau \geq 0$ need to be considered. Note that if $\tau \ll \Delta t$, the exponential term in Eq. (3) decays rapidly, and steady-state is approached quickly. In this case, for initial conditions far from steady-state, the loss term dominates the initial rate of evolution but then rapidly drops in magnitude as n is depleted and steady-state is approached. The $\Delta t/\tau \rightarrow \infty$ limit for an infinitely fast ODE corresponds to $\alpha \rightarrow 1$. Conversely, when $\tau \gg \Delta t$, then the exponential term in Eq. (3) slowly decays. The $\Delta t/\tau \rightarrow 0$ limit for an infinitely slow ODE corresponds to $\alpha \rightarrow \frac{1}{2}$. If the loss term is

identically equal to zero because $L_j=0$, then the solution for n is linear in time and the exact solution does not include the exponential term.

Given the demands of a reacting-flow application, α -QSS uses a predictor-corrector implementation. The predictor n_p takes the form

$$n_p = n_0 + \frac{\Delta t (P_0 - n_0/\tau_0)}{1 + \alpha_0 \Delta t/\tau_0} \quad (6)$$

and the corrector n_c is given by

$$n_c = n_0 + \frac{\Delta t (P^* - n_0/\tau^*)}{1 + \alpha^* \Delta t/\tau^*} \quad (7)$$

The index 0 indicates initial values, of P , τ , α and n . The averaged variables P^* , τ^* , and α^* are based on both the initial and the predicted values according to

$$\frac{1}{\tau^*} = \frac{1}{2} \left(\frac{1}{\tau_0} + \frac{1}{\tau_p} \right), \quad (8)$$

$$\alpha^* = \alpha (\Delta t/\tau^*), \quad \text{and} \quad (9)$$

$$P^* = \alpha^* P_p + (1 - \alpha^*) P_0 \quad (10)$$

where the index P indicates the ‘predicted’ values. The corrector step can be repeated using the previous corrector result as the new predicted value. Predictor-corrector methods of this type are single-point methods because information from only one a single time level is needed to initiate calculation of the solution at the next time level. The α -QSS method differs from previous QSS methods in its algebraic form (i.e., the use of the parameter α), the choice of α -weighted average for P , and the implementation as a predictor-corrector method. Previous methods calculate average values for P as arithmetic mean of P_0 and P_p (Radhakrishnan and Pratt, 1988; Verwer and Loon, 1994; Verwer and Simpson, 1995).

Numerical integration of troposphere photochemistry mechanism

F. Liu et al.

Title Page

Abstract

Introduction

Conclusions

References

Tables

Figures

◀

▶

◀

▶

Back

Close

Full Screen / Esc

Print Version

Interactive Discussion

**Numerical integration
of troposphere
photochemistry
mechanism**F. Liu et al.

[Title Page](#)[Abstract](#)[Introduction](#)[Conclusions](#)[References](#)[Tables](#)[Figures](#)[⏪](#)[⏩](#)[◀](#)[▶](#)[Back](#)[Close](#)[Full Screen / Esc](#)[Print Version](#)[Interactive Discussion](#)

The integrator CHEMEQ2 used in the current study is based on the α -QSS method (Mott, 1999; Mott and Oran, 2001). The accuracy of the integration is determined by the number of corrector iterations, N_c , and the time step, Δt . The timestep is calculated in the original way by CHEMEQ (Mott and Oran, 2001). The initially predicted values and final corrected values for species i are tested to see if they satisfy

$$\frac{\|n_{ic} - n_{ip}\|}{n_{ic}} \leq \varepsilon \quad (11)$$

for an user specified accuracy parameter. The parameter ε is defined as the predictor-corrector error tolerance. If Eq. (11) is not satisfied, the step is repeated with a smaller timestep. The parameter ε can be considered as the target relative error tolerance. In the current study, values of ε are taken as 0.10, 0.05, and 0.01, and unless otherwise specified, $N_c=1$.

4. Testing results

The comparison in this study is based upon the “Scenarios for Modelling of Multi-Phase Tropospheric Chemistry Version 2” (Poppe et al., 2001), which is available under: <http://www.fz-juelich.de/icg/icg-ii/ALLGEMEIN/cmdform.all.html>. Six scenarios are defined encompassing the remote planetary boundary layer over the continent (LAND) and the ocean (MARINE), the free troposphere (FREE), and three cases with varying burdens of anthropogenic and biogenic emissions (PLUME, URBAN, and URBAN/BIO) (Table 1). For our study only DRY Scenarios are used for the testing because the focus of this paper is to address gas-phase chemistry. CHEMEQ2 is used to calculate the five-day simulations, including both RACM and ReLACS. The prescribed photolysis frequencies and ‘exact’ references are the Sbox runs for the same scenarios. The Sbox includes the RACM mechanism and employs highly sophisticated VODE solver (Seefeld et al., 1999).

**Numerical integration
of troposphere
photochemistry
mechanism**F. Liu et al.

[Title Page](#)[Abstract](#)[Introduction](#)[Conclusions](#)[References](#)[Tables](#)[Figures](#)[◀](#)[▶](#)[◀](#)[▶](#)[Back](#)[Close](#)[Full Screen / Esc](#)[Print Version](#)[Interactive Discussion](#)

This test focuses on CHEMEQ2's ability to integrate ODEs efficiently at moderate accuracy on the one hand. The test examines the mechanism ReLACS's ability to predict ozone concentrations on the other. For this testing $\varepsilon=0.01$ and $N_C=1$ are fixed. In accordance with above purposes three modes (see Table 2) are implemented separately.

The simulations for O_3 , and ozone precursors NO , NO_2 , HO , organic peroxy radicals (RO_2) and peroxyacetyl nitrate (PAN) with the LAND, FREE, and PLUME cases are illustrated in Figs. 2 and 3. Since the RACM and ReLACS were designed and validated primarily for predicting ozone, agreement in ozone for the two mechanisms is expected even for the PLUME case with emissions. It can be seen in Fig. 4 that the differences of O_3 simulations for the three modes are increasing with simulation time but the maximum difference is less than 4 ppb(v). This is accurate enough considering the error tolerance of the O_3 observations. Despite this agreement in ozone, relatively significant differences for ozone precursors are seen between the two mechanisms. The difference in NO_2 between the two mechanisms is significantly high, but still less than 0.3 ppbv over 5 days, which might be caused by the over prediction of NO_2 by ReLACS during night. The study of Crassier et al. (2000) provides a detailed comparison of the mechanisms RACM and ReLACS.

The excellent agreement between the results from the different modes indicates that (1) the solver CHEMEQ2 is suitable for the numerical solution of the troposphere chemical balance equations, and (2) the mechanism ReLACS may replace RACM for ozone prediction.

In order to further investigate CHEMEQ2's sensitivity to the source strengths of NO and isoprene we use Mode B to simulate the URBAN and URBAN/BIO cases. In the URBAN case the emission strength of NO is as high as 5 times that of Q_0 in PLUME. The initial concentrations for NO , NO_2 , and CO are changed (Pope et al., 2001) and VOC emissions remain unchanged (see Table 3). This case is designed for polluted urban area with varying burdens of anthropogenic emissions. It can be seen in Fig. 5 that the simulations give high NO_2 concentrations over 5 days that lead to

**Numerical integration
of troposphere
photochemistry
mechanism**

F. Liu et al.

Title Page

Abstract

Introduction

Conclusions

References

Tables

Figures

⏪

⏩

◀

▶

Back

Close

Full Screen / Esc

Print Version

Interactive Discussion

very low production of ozone. Ozone production initially increases with the reduction of the emission strength of NO. The maximum ozone concentration reaches 178 ppb(v) when the emission strength of NO is approximately 2.5 times that of Q_0 . Then ozone production decreases with decreasing NO emission. Figure 6 gives the relation between O_3 and NO_x against different NO emission source strengths. Comparing with the PLUME case, the results indicate that at high NO_x concentration, the production of O_3 decreases with further NO_x emissions. This is expected when considering the contributions to the NO_x/VOC chemistry through emissions and initial concentrations for both the PLUME and the URBAN cases. The two cases have different emission strengths and initial concentrations of NO and VOCs, but both are very sensitive to these factors.

The URBAN/BIO case is intended to model the impact of an urban plume when passing a source of biogenic hydrocarbons. The first 60 h of URBAN/BIO is identical to the URBAN case, and the NO emission strength is $2.5 \cdot Q_0$. Then the anthropogenic VOC emissions are switched off and the biogenic emission (of isoprene) is switched on. Calculations continue until $t=120$ h. This simulation shows that the air parcels pick up anthropogenic emissions when passing an industrialized area and then transport them into a rural environment with biogenic emission. The production of O_3 slows after the anthropogenic VOC emissions end, and NO_x mixing ratio reduces rapidly afterwards (see Fig. 7).

5. Accuracy/Efficiency analysis

This section addresses trade-offs between the efficiency and accuracy of CHEMEQ2. The comparison focuses on numerical efficiency and accuracy with one chemical mechanism, RACM, eliminating differences due to the chemistry modules. For a comparison of the mechanisms RACM and ReLACS, the reader may refer to Gross et al. (2003) and Geiger et al. (2002).

5.1. Accuracy analysis

The relative difference between the simulations n_i by CHEMEQ2 and the ‘exact’ solutions n_{si} by VODE are calculated for each global time step for eight chosen species O_3 , NO , NO_2 , $HONO$, OH , $HCHO$, ALD , and PAN with the PLUME case. The relative difference with respect to VODE integration is defined as

$$RERR_i = \frac{n_{si} - n_i}{n_{si}} \quad (12)$$

In order to quantitatively identify the source of errors caused by internal parameter settings of the solver, a fixed global time step Δt_g of 30 min is used. The influence of Δt_g on accuracy and efficiency is discussed at the end of this section. Another way to assess the accuracy of solver is to compare the difference between the simulations and ‘exact’ solutions for all species at the endpoint, i.e. after the integration time of 132 h. As a global measure of this error, we calculate the “root mean square” (*r.m.s*) values by,

$$e_{r.m.s} = \sqrt{\frac{\sum_{i=1}^m RERR_i^2}{m}} \quad (13)$$

where $m=77$ is the number of species in RACM. Figure 8 shows the *RERR* for 77 species at the end point of integration. Even though the accuracy parameter $\varepsilon=0.1$ and $Nc=1$, the simulation of O_3 is accurate enough and $RERR_{O_3}$ is 7.793%. However the relative difference for HNO_3 , $HONO$, H_2O_5 , NO , NO_2 and NO_3 exceed 50%, and the accuracy of $HONO$ and N_2O_5 are worst among all the species. $RERR_{HONO}$ and $RERR_{N_2O_5}$ are 79.67% and 135%, respectively. When $\varepsilon=0.01$ and Nc remains 1, accuracy for all species is much improved. $RERR_{O_3}$, $RERR_{HONO}$ and $RERR_{N_2O_5}$ are 0.57%, 12.92% and 15.98%, respectively. If $\varepsilon=0.005$ and $Nc=5$ accuracy is further improved for all species but O_3 . $RERR_{O_3}$ is 0.59%. The maximum relative difference

Title Page

Abstract

Introduction

Conclusions

References

Tables

Figures

⏪

⏩

◀

▶

Back

Close

Full Screen / Esc

Print Version

Interactive Discussion

is 7.40% corresponding to $RERR_{\text{XYL}}$. $RERR_{\text{HONO}}$ and $RERR_{\text{N}_2\text{O}_5}$ are 0.95% and 1.92%, respectively.

In order to look into detailed variations of relative difference we present the variations of $RERR$ as a function of time for 8 species in Fig. 9. The analysis is carried out with four accuracy levels. The relative difference of O_3 is less than 10% even if ε is 0.1. But the $RERR$ s for other species such as NO_x , HONO, PAN, reach up to 60%, 90% and 30%, respectively. This can be expected, since the RACM is designed to model tropospheric chemistry with O_3 being the most important species. This also implies that it is not reasonable to evaluate a solver only with O_3 concentration. Figure 10 shows that the accuracy for all species is greatly improved as ε is decreased. When ε is reduced to 0.01 the relative difference of O_3 is less than 1% compared with the reference solutions. The $RERR$ s for all species are decreased considerably. The $RERR$ s for NO , NO_2 and HONO are less than 10%, and for HO, HCHO, ALD and PAN less than 5%. If a very accurate result is required and the added computational cost can be tolerated, in addition to lowering ε increasing Nc is dramatically effective. The case with $\varepsilon=0.005$ and $Nc=5$ gives more accurate simulations. However, further attempt to improve accuracy by decreasing ε or increasing Nc does not produce any significant change in the results because CHEMEQ2 was designed to provide moderately accurate solutions at low computation costs. In addition lowering ε is more efficient than increasing iterations Nc in improving accuracy if the CPU time is considered.

5.2. Trade offs between efficiency and accuracy analysis

The variation of root mean square $e_{r.m.s}$ and ε against CPU time are shown in Fig. 10. The smaller the $e_{r.m.s}$ the more expensive of computation is. The $e_{r.m.s}$ decreases, for example, from 24.61% to 2.33% as the CPU time increases from 0.47 s to 3.03 s. It can be seen in Fig. 11 that CHEMEQ2 is more efficient than VODE by at least a factor of 10 and is much faster especially at low level of accuracy. CHEMEQ2 is more expensive as the level of accuracy increases. The current tests suggest that VODE works better than CHEMEQ2 for $\varepsilon < 1\%$.

Numerical integration of troposphere photochemistry mechanism

F. Liu et al.

Title Page

Abstract

Introduction

Conclusions

References

Tables

Figures

◀

▶

◀

▶

Back

Close

Full Screen / Esc

Print Version

Interactive Discussion

**Numerical integration
of troposphere
photochemistry
mechanism**

F. Liu et al.

[Title Page](#)[Abstract](#)[Introduction](#)[Conclusions](#)[References](#)[Tables](#)[Figures](#)[⏪](#)[⏩](#)[◀](#)[▶](#)[Back](#)[Close](#)[Full Screen / Esc](#)[Print Version](#)[Interactive Discussion](#)

Both the accuracy and the efficiency are affected not only by internal parameters like ε and Nc but also by the global time step Δt_g . This is expected from the α -QSS method and the stiffness definition. The stiffness, as the characteristic of the system and not a specific problem, is highly influenced the time scales of the system. The time scale that ultimately governs the evolution of the solution must be compared to the time scale that limits the timestep of the numerical method. The box model is run as if it was used in each grid point in an operator splitting environment. At every new start for the integration of the solver, a global time step Δt_g is equal to the transport time step in a multiple processes reactive flow. The end integration for each Δt_g serves as the initial concentrations for the next restart, so the chemistry integrator gets a new initial-value problem at each global time step in each computational cell. Since the global time step is usually shorter than the time required for the slowest mode to become exhausted, the work required of the integration is largely independent of exactly how slow these modes are. A more accurate measure of how expensive the integration is will come from a comparison between the timestep required of the integrator and the global time step, not the ratio of the longest and shortest chemical time scales. One could increase the global time step as much as possible to improve the efficiency, particularly of multi-step integration schemes. There is, however, a loss of accuracy when the ratio $\Delta t/\Delta t_g$ is large, regardless of the choice of solver, because the physical conditions that effect the reaction rates are not well resolved. While one could decrease the global timestep to improve the accuracy, but the integration becomes more expensive. The trade-offs between accuracy and efficiency corresponding to the change of global time step is shown in Fig. 12. For three dimensional modeling the global time step must be generally fixed according to the time scale of the problem of interest. Therefore, the measures to improve accuracy by decreasing Δt_g as used in box model are not available in CTM, which is solved numerically according to a specific temporal and spatial resolution regarding to certain scales of interest.

The relative difference for most species except O_3 is influenced by Δt_g significantly in the box model. The major species like NO, NO_2 , HONO, PAN and N_2O_5 simulations

**Numerical integration
of troposphere
photochemistry
mechanism**

F. Liu et al.

Title Page

Abstract

Introduction

Conclusions

References

Tables

Figures

◀

▶

◀

▶

Back

Close

Full Screen / Esc

Print Version

Interactive Discussion

EGU

converge gradually to the reference results as decreasing of Δt_g from 3 h to 5 min. Obviously, when a too big global time step e.g. $\Delta t_g=3$ h, the simulations obtained by CHEMEQ2 will be too worse to be valid. In fact the largest global time step should not be bigger than 1 h, a typical time resolution of 3D global model.

5 In addition comparison of the two mechanisms RACM and ReLACS shows that the efficiency will be improved greatly if RACM is replaced by ReLACS. Taking the PLUME scenario as an example, the RACM consumes 0.3505 s ($\varepsilon=5\%$) and 1.6423 s ($\varepsilon=1\%$), respectively, while the ReLACS only takes 0.1802 s ($\varepsilon=5\%$) and 0.6710 s ($\varepsilon=1\%$), respectively, which gives a 50% CPU time saving.

10 6. Conclusions

A box model is developed and tested as a first application of the integration scheme CHEMEQ2, which has been developed based on the α -QSS algorithm, to the numerical integration of kinetic equations in tropospheric chemistry. Simulations are performed with the RACM and ReLACS gas-phase chemistry mechanisms under various atmospheric conditions and then compared with simulations using the VODE scheme. Both schemes are designed for process-split reacting-flow simulation.

15 The results demonstrate that the α -QSS scheme is efficient and relatively accurate in the solution of ODEs describing tropospheric chemistry. In the cases presented, when setting the relative error tolerance for CHEMEQ2 in the range from 5% to 1%, CHEMEQ2 agrees very well with VODE with a *r.m.s.* < 5% for all species in RACM as well as in ReLACS. CHEMEQ2 is at least 10-times faster than VODE when using the same global time step. CHEMEQ2, therefore, gives a comparable level of accuracy with a lower computational cost than VODE at moderate accuracy. VODE outperforms CHEMEQ2 when the higher level of accuracy ($\varepsilon < 1\%$) is required. Since hydrodynamic error in multi-processes system rarely smaller than a few percent, CHEMEQ2 is the better candidate for integrating chemical ODEs coupled with expensive CTMs. The accuracy constraint in CHEMEQ2 does not measure the error directly but measures the

20

25

correction to the predicted values provided by the corrector step. Therefore, experience with a particular mechanism is necessary to know how to set the optional parameters in CHEMEQ2 in order to produce a given level of accuracy in the solution. Future work will determine if these parameters are consistent between the box model and full three-dimensional simulations and whether CHEMEQ2 outperforms other solvers for 3-D CTM.

The ReLACS will save at least 50% CPU time compared against the RACM under the same conditions when the chemistry integration stands alone. The study also shows that the trade offs between accuracy and efficiency is influenced by the global time step because it is related to the choice of the chemical time step for the integration.

Choosing a smaller global time step leads to a more accurate but more expensive integration. Conversely, this suggests that one should increase the global time step as much as possible to improve the efficiency. In practice, the global time step is chosen to accurately couple the various processes present in the simulation. Therefore, although the chemistry integration would be less expensive using a larger global time step, this time step is often set by other requirements in a reacting flow simulation. The solution approach must employ the most efficient chemistry integrator that meets the accuracy requirements of the application, subject to this time step constraint.

For the modeling study of ozone trends over the regions of interest the efficiency of CTM is very important due to limited computational power but moderate accuracy is sufficient given the accuracy of other components in the model and the uncertainty in available experimental data. The solver CHEMEQ2 and the chemistry mechanism ReLACS will be the basic components for developing our next generation CTM for simulating long term change of ozone over the regions of interest.

**Numerical integration
of troposphere
photochemistry
mechanism**

F. Liu et al.

Title Page

Abstract

Introduction

Conclusions

References

Tables

Figures

◀

▶

◀

▶

Back

Close

Full Screen / Esc

Print Version

Interactive Discussion

No	RACM	RACM and ReLACS species list		Definition
		No	ReLACS	
	<i>Oxidants</i>			<i>Stable Inorganic Compounds</i>
1	O ₃	1	O ₃	Ozone
2	H ₂ O ₂	2	H ₂ O ₂	Hydrogen peroxide
	<i>Nitrogenous compound</i>			
3	NO	3	NO	nitric oxide
4	NO ₂	4	NO ₂	Nitrogen dioxide
5	NO ₃	5	NO ₃	Nitrogen trioxide
6	N ₂ O ₅	6	N ₂ O ₅	Dinitrogen pentoxide
7	HONO	7	HONO	nitrous acid
8	HNO ₃	8	HNO ₃	Nitric acid
9	HNO ₄	9	HNO ₄	pernitric acid
	<i>Sulfur compounds</i>			
10	SO ₂	10	SO ₂	sulphur dioxide
11	SULF			sulphuric acid
	<i>Carbon oxides</i>			
12	CO	11	CO	carbon monoxide
13	CO ₂			carbon dioxide
				<i>Abundant Stable Species</i>
14	N ₂			Nitrogen
15	O ₂			Oxygen
16	H ₂ O			Water
17	H ₂			Hydrogen
				<i>Inorganic Short-Lived Intermediates</i>
18	O ³ P			ground state atom
19	O ¹ D			excited state oxygen atom
	<i>Odd hydrogen</i>			
20	HO			hydroxyl radical
21	HO ₂	12	HO ₂	hydroperoxy radical
	<i>Alkanes</i>			
22	CH ₄	13	CH ₄	Methane
23	ETH	14	ETH	Ethane
24	HC3	15	ALKA	alkanes, alcohols, esters, and alkynes ¹
25	HC5			alkanes, alcohols, esters, and alkynes ²
26	HC8			alkanes, alcohols, esters, and alkynes ³
	<i>Alkenes</i>			
27	ETE	16	ETE	Ethane
28	OLT			Terminal alkenes
29	OLI			Internal alkenes
30	DIEN			Butadiene and other anthropogenic dienes

Numerical integration of troposphere photochemistry mechanism

F. Liu et al.

Title Page

Abstract

Introduction

Conclusions

References

Tables

Figures

◀

▶

◀

▶

Back

Close

Full Screen / Esc

Print Version

Interactive Discussion

Numerical integration of troposphere photochemistry mechanism

F. Liu et al.

RACM and ReLACS species list				
No	RACM	No	ReLACS	Definition
<i>Stable biogenic alkenes</i>				
31	ISO	17	BIO	Isoprene
32	API			α -pinene and other cyclic terpenes with one double bond
33	LIM			d-limonene and other cyclic diene-terpenes
<i>Aromatics</i>				
34	TOL	18	ARO	Toluene
35	XYL			Xylene
36	CSL			cresol and other aromatics
<i>Carbonyls</i>				
37	HCHO	19	HCHO	Formaldehyde
38	ALD	20	ALD	acetaldehyde and higher aldehydes
39	KET	21	KET	Ketones
40	GLY	22	CARBO	Glyoxal
41	MGLY			methyglyoxal and other α -carbonyl aldehydes
42	DCB			unsaturated dicarbonyls
43	MACR			metacrolein and other unsaturated monoaldehydes
44	UDD			unsaturated dihydroxy dicarbonyl
45	HKET			hydroxyl ketone
<i>Organic nitrogen</i>				
46	ONIT	23	ONIT	organic nitrate
47	PAN	24	PAN	peroxyacetyl nitrate and higher saturated PANs
48	TPAN			unsaturated PANs
<i>Organic peroxides</i>				
49	OP1	25		methyl hydrogen peroxide
50	OP2	26		higher organic peroxides
51	PAA			peroxyacetic acid and higher analogs
<i>Organic acids</i>				
52	ORA1			formic acid
53	ORA2	27		acetic and higher acids
<i>Peroxy radicals from alkanes</i>				
54	MO2	28	MO2	methyl peroxy radical
55	ETHP	29	ALKAP	peroxy radicals formed from ALKA
56	HC3P			peroxy radicals formed from HC3
57	HC5P			peroxy radicals formed from HC5
58	HC8P			peroxy radicals formed from HC8
<i>Peroxy radicals from alkenes</i>				
59	ETEP	30	ALKEP	peroxy radicals formed from ALKE
60	OLTP			peroxy radicals formed from OLT
61	OLIP			peroxy radicals formed from OLI

[Title Page](#)
[Abstract](#)
[Introduction](#)
[Conclusions](#)
[References](#)
[Tables](#)
[Figures](#)
[⏪](#)
[⏩](#)
[◀](#)
[▶](#)
[Back](#)
[Close](#)
[Full Screen / Esc](#)
[Print Version](#)
[Interactive Discussion](#)

Numerical integration of troposphere photochemistry mechanism

F. Liu et al.

No	RACM	RACM and ReLACS species list		Definition
		No	ReLACS	
<i>Peroxy radicals from biogenic alkenes</i>				
62	ISOP	31	PHO	peroxy radicals formed from BIO
63	APIP			peroxy radicals formed from API
64	LIMP			peroxy radicals formed from LIM
<i>Radicals produced from aromatics</i>				
65	PHO	32	PHO	phenoxy radical and similar radicals
66	ADDT	33	ADD	aromatic-OH adduct from ADD
67	ADDX			aromatic-OH adduct from XYL
68	ADDC			aromatic-OH adduct from CSL
69	TOLP	34	AROP	peroxy radicals formed from ARO
70	XYLP			peroxy radicals formed from XYL
71	CSLP			peroxy radicals formed from CSL
<i>Peroxy radicals with carbonyl group</i>				
72	ACO ₃	35	CARBOP	acetyl peroxy and higher saturated acyl peroxy radicals
73	TCO ₃			unsaturated acyl peroxy radicals
74	KETP			peroxy radicals formed from KET
<i>Other peroxy radicals</i>				
75	OLNN	36	OLN	NO ₃ -alkene adduct
76	OLND			NO ₃ -alkene adduct reacting via decomposition
77	XO ₂	37	XO ₂	Accounts for additional NO to NO ₂ conversions

¹ with HO rate constant less than $3.4 \times 10^{-12} \text{ cm}^3 \text{ s}^{-1}$

² with HO rate constant between 3.4×10^{-12} and $6.8 \times 10^{-12} \text{ cm}^3 \text{ s}^{-1}$

³ with HO rate constant greater than $6.8 \times 10^{-12} \text{ cm}^3 \text{ s}^{-1}$

- 5 *Acknowledgements.* We thank W. Stockwell for providing RACM and access to his Sbox model. We also thank C. Mari for providing ReLACS and helpful discussion. We are grateful for the suggestion from D. Poppe and Y. Liu.

References

- 10 Avro, C. G.: A stiff ODE solver for the equations of chemical kinetics, *Computer Physics Communications*, 97, 304–314, 1996.
- Brown, P. N., Byrne, G. D., and Hindmarsh, A. C.: VODE: A variable coefficient ODE Solver, *SIAM J. Sci. Stat. Comput.*, 10, 1038–1051, 1989.

[Title Page](#)
[Abstract](#)
[Introduction](#)
[Conclusions](#)
[References](#)
[Tables](#)
[Figures](#)
[⏪](#)
[⏩](#)
[◀](#)
[▶](#)
[Back](#)
[Close](#)
[Full Screen / Esc](#)
[Print Version](#)
[Interactive Discussion](#)

**Numerical integration
of troposphere
photochemistry
mechanism**

F. Liu et al.

[Title Page](#)[Abstract](#)[Introduction](#)[Conclusions](#)[References](#)[Tables](#)[Figures](#)[⏪](#)[⏩](#)[◀](#)[▶](#)[Back](#)[Close](#)[Full Screen / Esc](#)[Print Version](#)[Interactive Discussion](#)

- Geiger, H., Barnes I., Becker, K. H., et al.: Chemical mechanism development: Laboratory studies and model application, *J. Atmos. Chem.*, 42, 323–357, 2002.
- Crassier, V., Suhre, K., Tulet, P., and Rosset, R.: Development of a reduced chemical scheme for use in mesoscale meteorological model, *Atmos. Environ.*, 34, 2633–2644, 2000.
- 5 Derwent, R. G. and Jenkin, M. E.: Hydrocarbons and the long-range transport of ozone and PAN across Europe, *Atmos. Environ.*, 25A(8), 1661–1678, 1991.
- Derwent, R. G., Jenkin, M. E., Saunders, S. M., and Pilling, M. J.: Photochemical ozone creation potentials for organic compounds in northwest Europe calculated with a master chemical mechanism, *Atmos. Environ.*, 32, 2429–2441, 1998.
- 10 Gear, C. W.: Numerical initial value problems in ordinary differential equations, Prentice-Hall, Englewood Cliffs, New Jersey, 1971.
- Gery, M. W., Whitten, G. Z., Killus, J. P., and Dodge, M. C.: A photochemical kinetics mechanism for urban and regional scale computer modelling, *J. Geophys. Res.*, 94, 12 925–12 956, 1989.
- 15 Gross, A. and Stockwell, W.: Comparison of EMEP, RADM2 and RACM Mechanisms, *J. Atmos. Chem.*, 44, 151–170, 2003.
- Hairer, E. and Wanner, G.: Solving ordinary differential equations II. Stiff and Differential-Algebraic Problems, Springer-Verlag, Berlin, 1991.
- Hertel, O., Berkowicz, R., Christensen, J., and Hov, Ø.: Test of two chemical schemes for use in atmospheric transport chemistry models, *Atmos. Environ.*, 27A, 2591–2611, 1993.
- 20 Hindmarsh, A. C.: ODEPACK, a systematic collection of ODE solvers, in: Numerical methods for scientific computation, edited by: Stepleman, R. S., North Holland, New York, 55–64, 1983.
- Hindmarsh, A. C. and Norsett, S. P.: KRYSI, An ODE Solver Combining a Semi-Implicit Runge-Kutta Method and a Preconditioned Krylov Method, LLNL report UCID-21422, 1988.
- 25 Jay, L. O., Sandu, A., Porta, F. A., and Carmichael, G. R.: Improved Quasi-Steady-State-Approximation methods for atmospheric chemistry integration, *SIAM Journal of Scientific Computing*, 18, 182–202, 1997.
- Jenkin, M. E., Saunders, S. M., and Pilling, M. J.: The Tropospheric degradation of volatile organic compounds: A protocol for mechanism development, *Atmos. Environ.*, 31, 81–104, 1997.
- 30 Jimenez, P., Baldasano, J. M., and Dabdub, D.: Comparison of photochemical mechanisms for air quality modelling, *Atmos. Environ.*, 37, 4179–4194, 2003.

**Numerical integration
of troposphere
photochemistry
mechanism**F. Liu et al.

[Title Page](#)[Abstract](#)[Introduction](#)[Conclusions](#)[References](#)[Tables](#)[Figures](#)[⏪](#)[⏩](#)[◀](#)[▶](#)[Back](#)[Close](#)[Full Screen / Esc](#)[Print Version](#)[Interactive Discussion](#)

- Kohlmann, J. P. and Poppe, D.: The tropospheric gas-phase degradation of NH_3 and its impact on the formation of N_2O and NO_x . *J. Atmos. Chem.*, 32, 397–415, 2003.
- Kuhn, M., Bultjes, P. J. H., Poppe, D., et al.: Intercomparison of the gas-phase chemistry in several chemistry and transport models, *Atmos. Environ.*, 32(4), 693–709, 1998.
- 5 Lorenzini, R. and Passoni, L.: Test of numerical methods for the integration of kinetic equations in tropospheric chemistry, *Computer Physics Communications*, 117, 241–249, 1999.
- Lurmann, F. W., Lloyd, A. C., and Atkinson, R.: A chemical mechanism for use in long-range transport/acid deposition computer modelling, *J. Geophys. Res.*, 91, 10 905–10 936, 1986.
- Mott, D. R., Oran, E. S., and van Leer, B.: A Quasi-Steady-State Solver for the Stiff Ordinary
10 Differential Equations of Reaction Kinetics, *Journal of Computational Physics*, 164, 407–428, 2000.
- Mott, D. R. and Oran, E. S.: CHEMEQ2: A solver for the stiff ordinary differential equations of chemical kinetics, *NRL Memorandum Report No. 6400-01-8553*, 2001.
- Oran, E. S. and Boris, J. P.: *Numerical simulation of reactive flow*, Elsevier Science Publishing Co., Inc., New York, 1987.
- 15 Oran, E. S. and Boris, J. P.: *Numerical simulation of reactive flow*, Elsevier Science Publishing Co., Inc., New York, 2000.
- Poppe, D., Andersson-Sköld, Y., Baart, A., Bultjes, P. J. H., et al.: Gas-phase reactions in atmospheric chemistry and transport models: a model intercomparison, *EUROTRAC Report*,
20 1996.
- Poppe, D., Aumont, B., Evens, B., et al.: Scenarios for modeling multiphase tropospheric chemistry, *J. Atmos. Chem.*, 40, 77–86, 2001.
- Radhakrishnan, K. and Pratt, D. T.: Fast algorithm for calculating chemical kinetics in turbulent reacting flow, *Combustion Science and Technology*, 58, 155–176, 1988.
- 25 Radhakrishnan, K. and Hindmarsh, A. C.: Description and Use of LSODE, the Livermore Solver for Ordinary Differential Equations, LLNL report UCRL-ID-113855, 1993.
- Sandu, A., Potra, F. A., Damian, V., and Carmichael, G. R.: Efficient implementation of fully implicit methods for atmospheric chemistry kinetics. *Reports on computational mathematics*, No. 79/1995, The Uni. of Iowa, 1995.
- 30 Sandu, A., Verwer, J. G., van Loon, M., Carmichael, G. R., Potra, F. A., Dabdub, D., and Seinfeld, J. H.: Benchmarking stiff ODE solvers for atmospheric chemistry problems I: Implicit versus explicit, *NM-R9614*, 1996.
- Saylor, R. D. and Ford, G. D.: On the comparison of numerical methods for the integration

of kinetic equations in atmospheric chemistry and transport models, *Atmos. Environ.*, 29, 2585–2593, 1995.

Seefeld, S. and Stockwell, W.: First-order sensitivity analysis of models with time-dependent parameters: an application to PAN and ozone, *Atmos. Environ.*, 33, 2941–2953, 1999.

5 Shyan-Shu Shield, D., Chang, Y., and Carmichael, G. R.: The evaluation of numerical techniques for solution of stiff ODE arising from chemical kinetic problems, *Envir. Sof.*, 3, 28–38, 1988.

Simpson, D., Andersson-Sköld, Y., and Jenkin, M. E.: Updating the chemical scheme for the EMEP MSC-W oxidant model: current status, EMEP MSC-W Note 2/93, Norwegian Meteorological Institute, Oslo, Norway, 1993.

10 Stockwell, W. R., Middleton, P., Chang, J. S., and Tang, X.: The second generation regional acid deposition model chemical mechanism for regional air quality modelling, *J. Geophys. Res.*, 95, 16 343–16 367, 1990.

Stockwell, W. R. and Kley, D.: The Euro-RADM Mechanism: A gas-phase chemical mechanism for European air quality studies, Forschungszentrum Jülich GmbH (KFA), Jülich, Germany, 1994.

15 Stockwell, W. R., Krichner, F., Kuhn, M., and Seefeld, S.: A new mechanism for regional atmospheric chemistry modeling, *J. Geophys. Res.*, 102(D22), 25 847–25 879, 1997.

Verwer, J. G. and van Loon, M.: An evaluation of explicit Psuedo-Steady-State Approximation Schemes for Stiff ODE Systems from Chemical Kinetics, *Journal of Computational Physics*, 20 113, 347–352, 1994.

Verwer, J. G. and Simpson, D.: Explicit methods for stiff ODEs from atmospheric chemistry, *Applied Numerical Mathematics*, 18, 413–430, 1995.

Verwer, J. G., Blom, J. G., van Loon, M., and Spee, E. J.: A comparison of stiff ODE solvers for atmospheric chemistry problems, NM-R9505, 1995.

25 Young, T. R.: CHEMEQ – A subroutine for solving stiff ordinary differential equations, NRL Memorandum Report No. 4091, 1980.

Young, T. R. and Boris, J. P.: A numerical technique for solving stiff ordinary differential equations associated with the chemical kinetics of reactive-flow problems, *J. Phys. Chem.*, 81, 2424–2427, 1977.

**Numerical integration
of troposphere
photochemistry
mechanism**

F. Liu et al.

Title Page

Abstract

Introduction

Conclusions

References

Tables

Figures

◀

▶

◀

▶

Back

Close

Full Screen / Esc

Print Version

Interactive Discussion

Numerical integration of troposphere photochemistry mechanism

F. Liu et al.

Table 1. Scenarios description.

Scenarios	Short description	Emissions	j-values
LAND	continental planetary boundary layer with a low burden of pollutants	no	Prescribed
MARINE	marine boundary layer	no	Prescribed
FREE	middle troposphere	no	Prescribed
PLUME	moderately polluted PBL	yes	Prescribed
URBAN	polluted PBL	yes	Prescribed
URBAN/BIO	URBAN plume with biogenic impact	yes	Prescribed

Title Page

Abstract

Introduction

Conclusions

References

Tables

Figures

⏪

⏩

◀

▶

Back

Close

Full Screen / Esc

Print Version

Interactive Discussion

**Numerical integration
of troposphere
photochemistry
mechanism**F. Liu et al.

[Title Page](#)[Abstract](#)[Introduction](#)[Conclusions](#)[References](#)[Tables](#)[Figures](#)[I◀](#)[▶I](#)[◀](#)[▶](#)[Back](#)[Close](#)[Full Screen / Esc](#)[Print Version](#)[Interactive Discussion](#)**Table 2.** Modes for simulation.

Mode	Mechanism	Solver	Note
A	RACM	VODE	reference
B	RACM	CHEMEQ2	Tests
C	ReLACS	CHEMEQ2	Tests

Numerical integration of troposphere photochemistry mechanism

F. Liu et al.

Table 3. Emission data for cases PLUME, URBAN, and URBAN/BIO.

Compounds	Emission strength (ppb/min)	Compounds	Emission strength (ppb/min)
ALD	0.36200E-04	KET	0.31200E-03
CO	0.56500E-02	NO	0.25900E-02~0.012950 ^a
TE	0.45600E-03	OLI	0.18800E-03
ETH	0.24100E-03	OLT	0.21900E-03
HC3	0.29100E-02	SO2	0.51800E-03
HC5	0.76900E-03	TOL	0.57300E-03
HC8	0.45500E-03	XYL	0.51900E-03
HCHO	0.13900E-03		

^a For the PLUME case the NO emission strength, denote Q_0 , is 0.25900E-02 (ppb/min). The strength is 5 times of Q_0 ($Q=5 * Q_0=0.012950$ ppb/min) for URBAN and URBAN/BIO cases.

[Title Page](#)
[Abstract](#)
[Introduction](#)
[Conclusions](#)
[References](#)
[Tables](#)
[Figures](#)
[Back](#)
[Close](#)
[Full Screen / Esc](#)
[Print Version](#)
[Interactive Discussion](#)

**Numerical integration
of troposphere
photochemistry
mechanism**F. Liu et al.

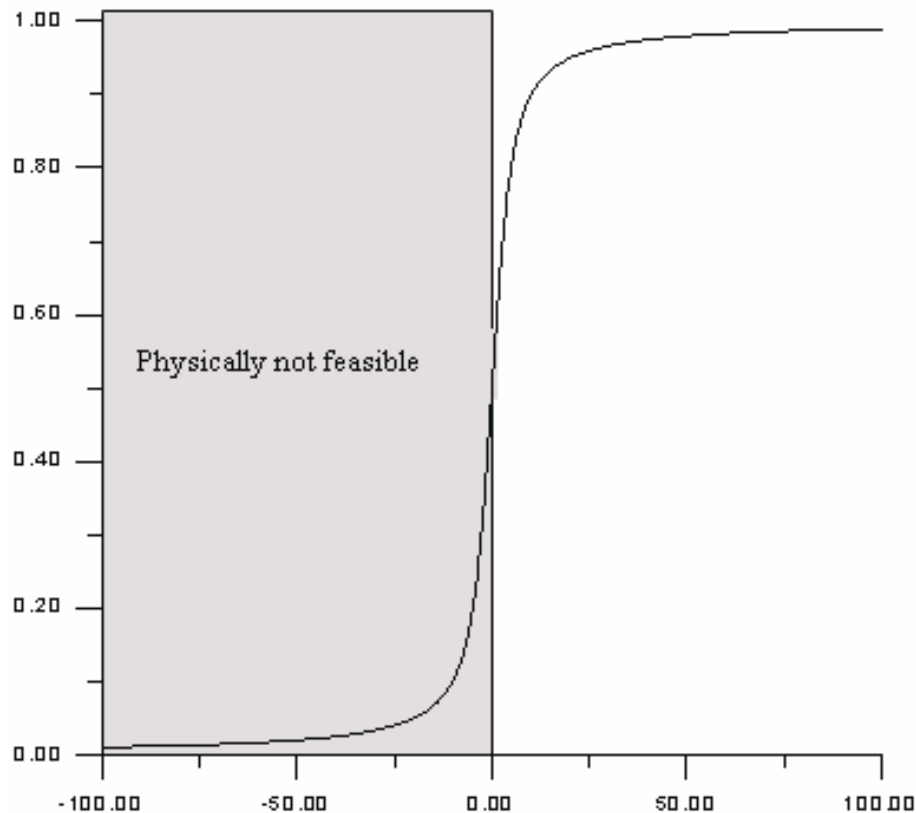


Fig. 1. The parameter α (y-coordinator) as a function of $\Delta t / \tau$ (abscissa).

[Title Page](#)[Abstract](#)[Introduction](#)[Conclusions](#)[References](#)[Tables](#)[Figures](#)[◀](#)[▶](#)[◀](#)[▶](#)[Back](#)[Close](#)[Full Screen / Esc](#)[Print Version](#)[Interactive Discussion](#)

Numerical integration
of troposphere
photochemistry
mechanism

F. Liu et al.

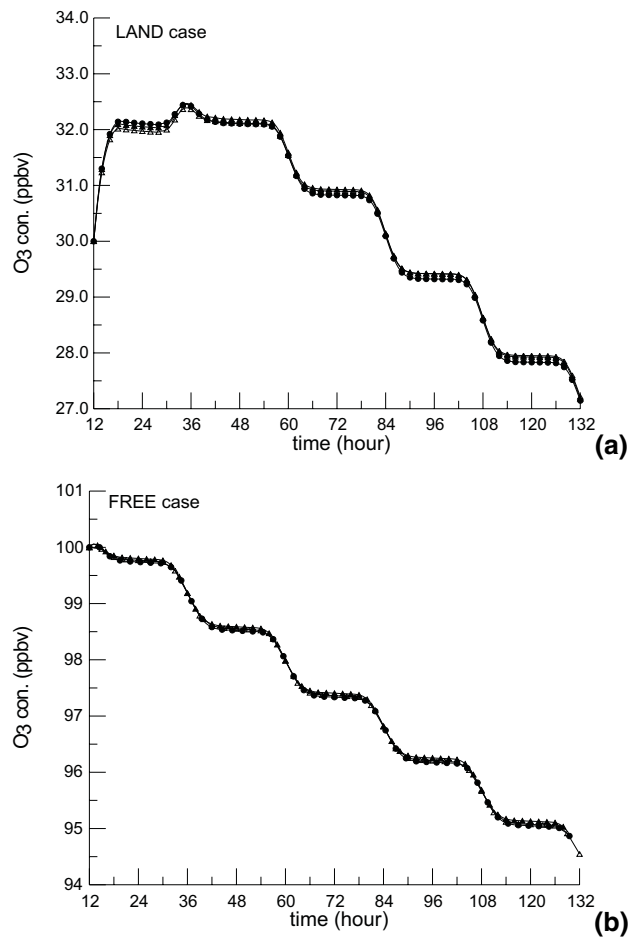


Fig. 2. Mixing ratio for O₃ as function of time for the LAND (a) and the FREE (b) cases from different modes which are described in Table 2. The simulations start at noon with output every 30 min (●: Mode A; △: Mode B; ▲: Mode C).

[Title Page](#)[Abstract](#)[Introduction](#)[Conclusions](#)[References](#)[Tables](#)[Figures](#)[◀](#)[▶](#)[◀](#)[▶](#)[Back](#)[Close](#)[Full Screen / Esc](#)[Print Version](#)[Interactive Discussion](#)

Numerical integration
of troposphere
photochemistry
mechanism

F. Liu et al.

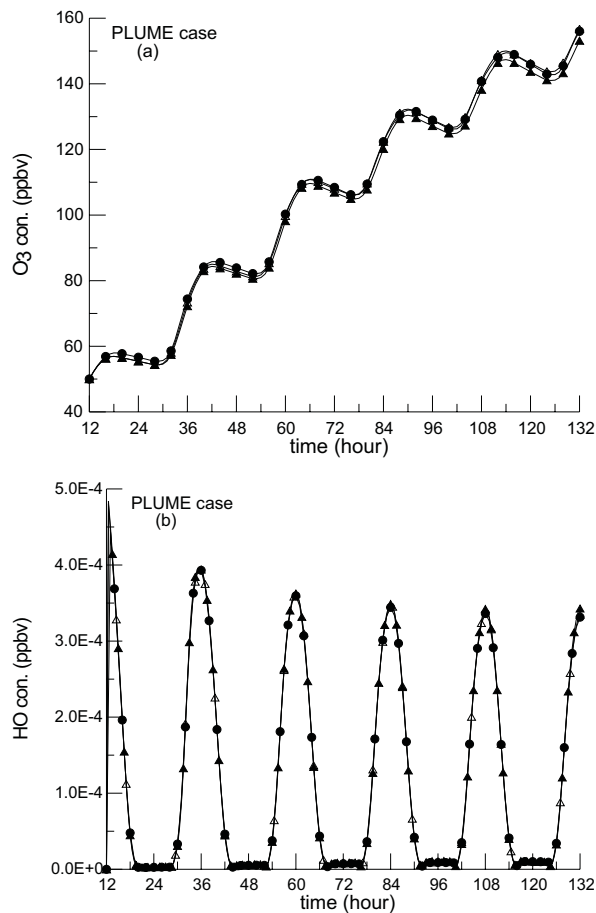


Fig. 3. Mixing ratio for O₃ (a), HO (b), NO (c), NO₂ (d), PAN (e) and RO₂ (f) as function of time for the PLUME case with three Modes which are described in Table 2. The simulations start at noon with output every 30 min (-●- : Mode A; -△- : Mode B; -▲- : Mode C).

[Title Page](#)[Abstract](#)[Introduction](#)[Conclusions](#)[References](#)[Tables](#)[Figures](#)[◀](#)[▶](#)[◀](#)[▶](#)[Back](#)[Close](#)[Full Screen / Esc](#)[Print Version](#)[Interactive Discussion](#)

Numerical integration
of troposphere
photochemistry
mechanism

F. Liu et al.

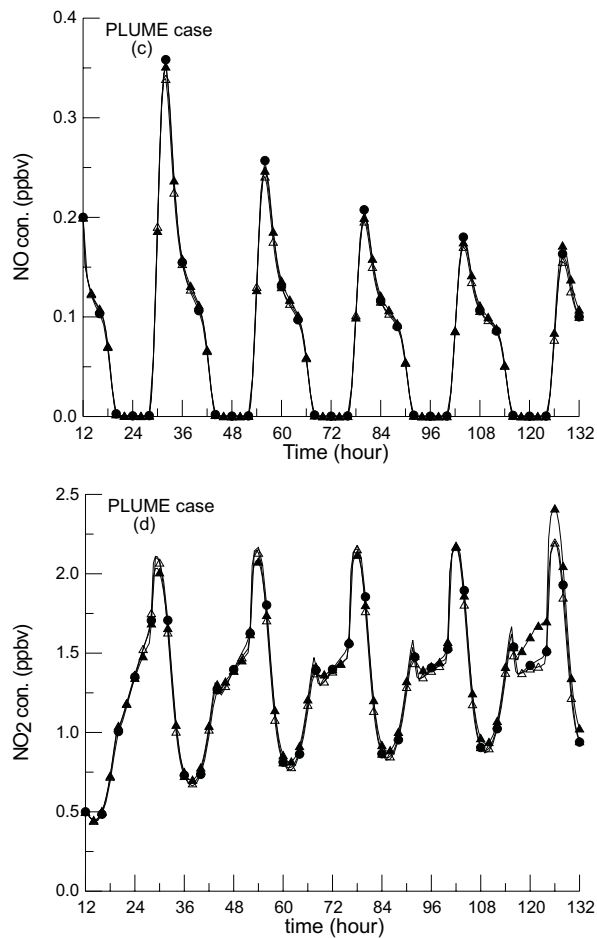


Fig. 3. Continued.

[Title Page](#)[Abstract](#)[Introduction](#)[Conclusions](#)[References](#)[Tables](#)[Figures](#)[◀](#)[▶](#)[◀](#)[▶](#)[Back](#)[Close](#)[Full Screen / Esc](#)[Print Version](#)[Interactive Discussion](#)

**Numerical integration
of troposphere
photochemistry
mechanism**

F. Liu et al.

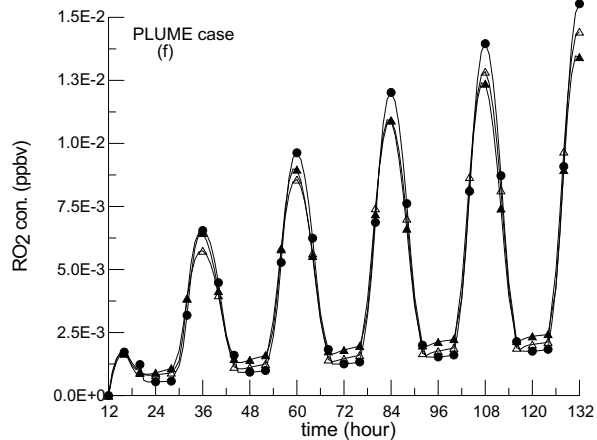
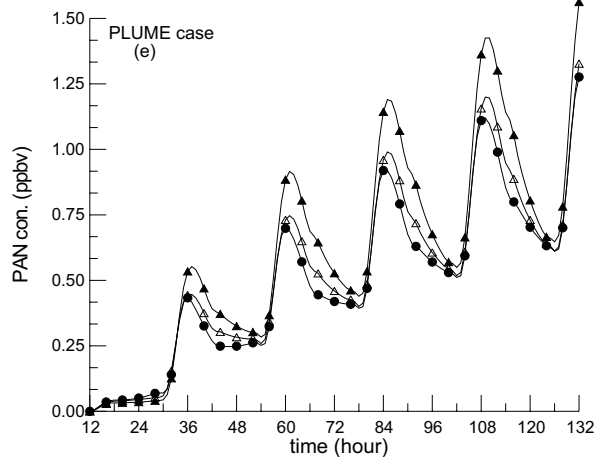


Fig. 3. Continued.

[Title Page](#)[Abstract](#)[Introduction](#)[Conclusions](#)[References](#)[Tables](#)[Figures](#)[◀](#)[▶](#)[◀](#)[▶](#)[Back](#)[Close](#)[Full Screen / Esc](#)[Print Version](#)[Interactive Discussion](#)

Numerical integration
of troposphere
photochemistry
mechanism

F. Liu et al.

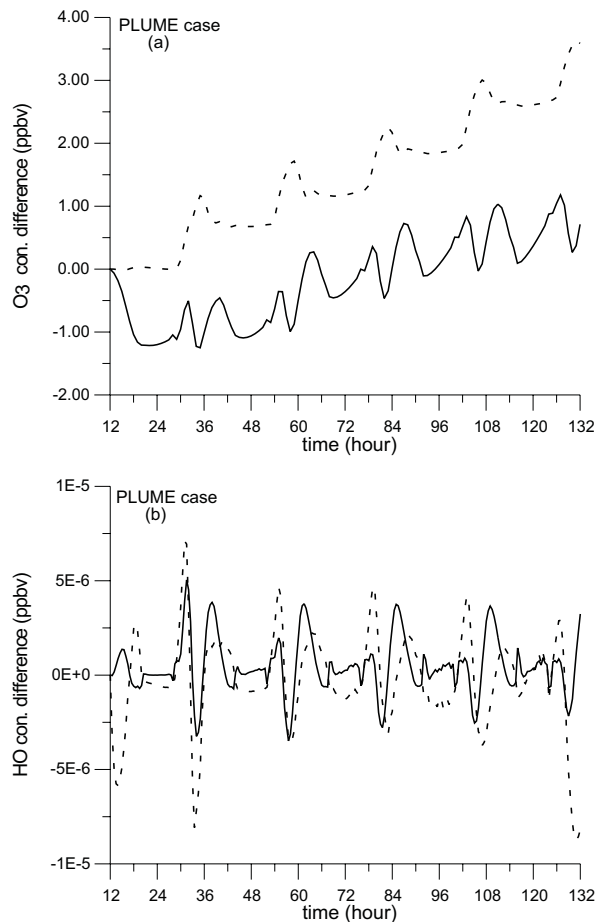


Fig. 4. The concentration difference between Modes for O₃ (a), HO (b), NO (c), NO₂ (d), PAN (e) and RO₂ (f) as function of time for the PLUME case. The three Modes are described in Table 2. The simulations start at noon with output every 30 min (solid line: Mode B – Mode A; dashed line: Mode B – Mode C).

[Title Page](#)[Abstract](#)[Introduction](#)[Conclusions](#)[References](#)[Tables](#)[Figures](#)[◀](#)[▶](#)[◀](#)[▶](#)[Back](#)[Close](#)[Full Screen / Esc](#)[Print Version](#)[Interactive Discussion](#)

**Numerical integration
of troposphere
photochemistry
mechanism**

F. Liu et al.

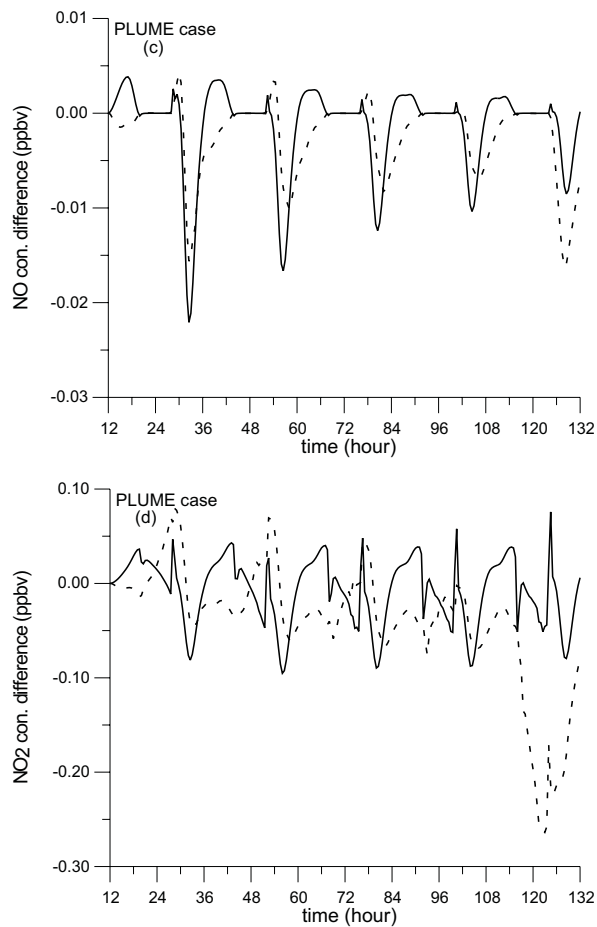
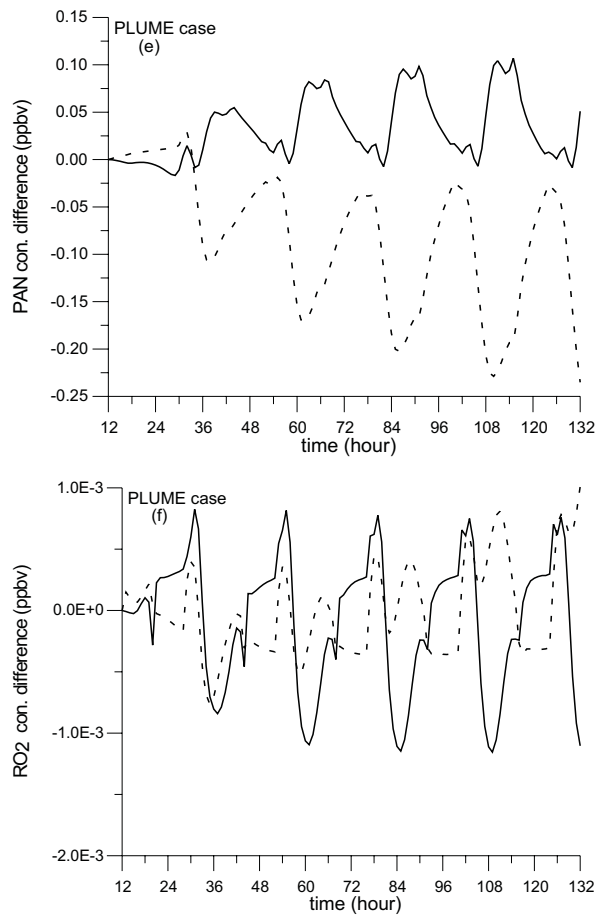


Fig. 4. Continued.

[Title Page](#)[Abstract](#)[Introduction](#)[Conclusions](#)[References](#)[Tables](#)[Figures](#)[◀](#)[▶](#)[◀](#)[▶](#)[Back](#)[Close](#)[Full Screen / Esc](#)[Print Version](#)[Interactive Discussion](#)

**Numerical integration
of troposphere
photochemistry
mechanism**

F. Liu et al.

**Fig. 4.** Continued.[Title Page](#)[Abstract](#)[Introduction](#)[Conclusions](#)[References](#)[Tables](#)[Figures](#)[◀](#)[▶](#)[◀](#)[▶](#)[Back](#)[Close](#)[Full Screen / Esc](#)[Print Version](#)[Interactive Discussion](#)

Numerical integration of troposphere photochemistry mechanism

F. Liu et al.

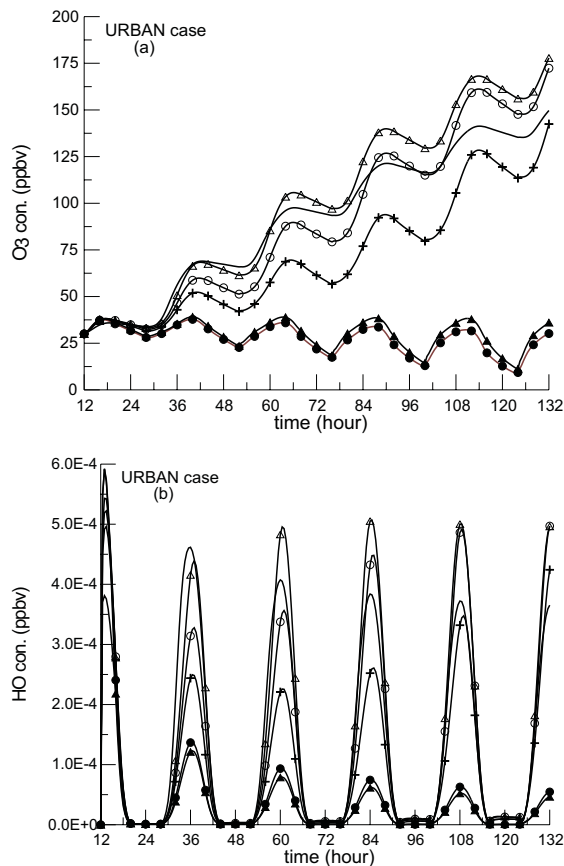


Fig. 5. Mixing ratios of O₃ (a), HO (b), NO (c), NO₂ (d), PAN (e) and RO₂ (f) as function of time for the URBAN case with different NO emission strengths. The emissions are described in Table 3. The simulations start at noon with output every 30 min. The Q_0 of 2.5900×10^{-3} ppb min^{-1} is the base NO emission strength as prescribed in the PLUME case (Solid line: Q_0 ; Δ : $2.5 \cdot Q_0$; $-$: $3.0 \cdot Q_0$; $+$: $3.5 \cdot Q_0$; \bullet : $5.0 \cdot Q_0$; \blacktriangle : $5.0 \cdot Q_0$ with Mode A).

Title Page

Abstract

Introduction

Conclusions

References

Tables

Figures

◀

▶

◀

▶

Back

Close

Full Screen / Esc

Print Version

Interactive Discussion

**Numerical integration
of troposphere
photochemistry
mechanism**

F. Liu et al.

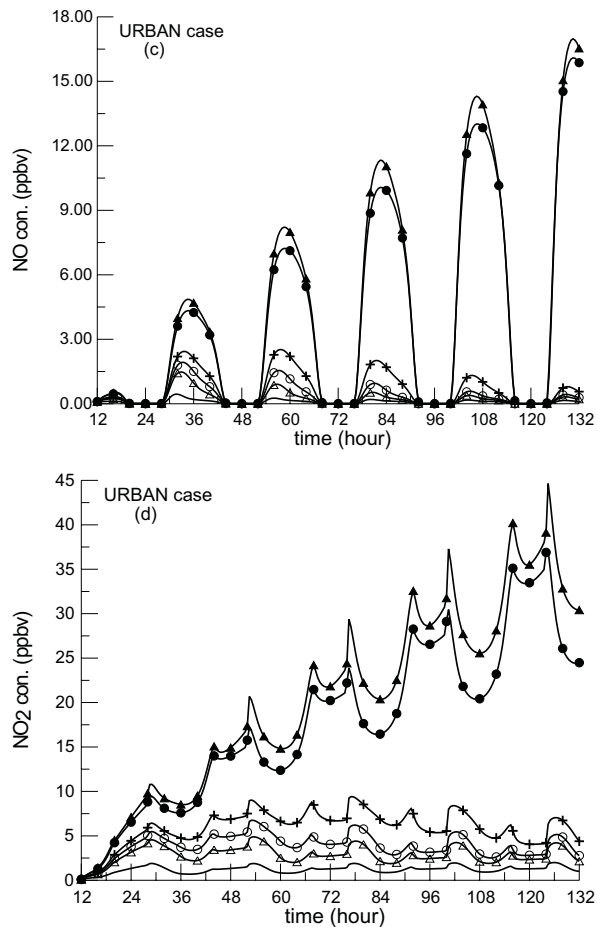


Fig. 5. Continued.

[Title Page](#)[Abstract](#)[Introduction](#)[Conclusions](#)[References](#)[Tables](#)[Figures](#)[◀](#)[▶](#)[◀](#)[▶](#)[Back](#)[Close](#)[Full Screen / Esc](#)[Print Version](#)[Interactive Discussion](#)

Numerical integration
of troposphere
photochemistry
mechanism

F. Liu et al.

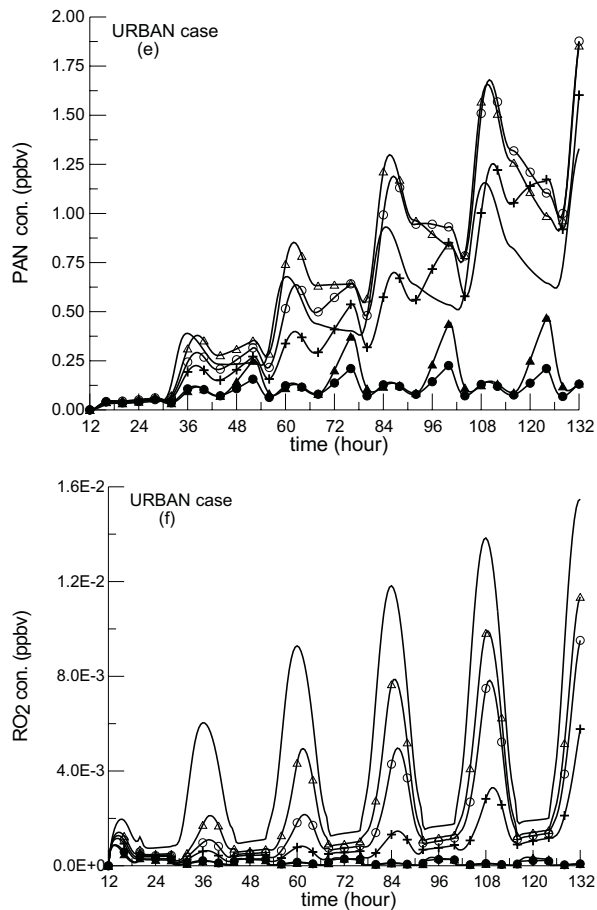


Fig. 5. Continued.

[Title Page](#)[Abstract](#)[Introduction](#)[Conclusions](#)[References](#)[Tables](#)[Figures](#)[◀](#)[▶](#)[◀](#)[▶](#)[Back](#)[Close](#)[Full Screen / Esc](#)[Print Version](#)[Interactive Discussion](#)

**Numerical integration
of troposphere
photochemistry
mechanism**F. Liu et al.

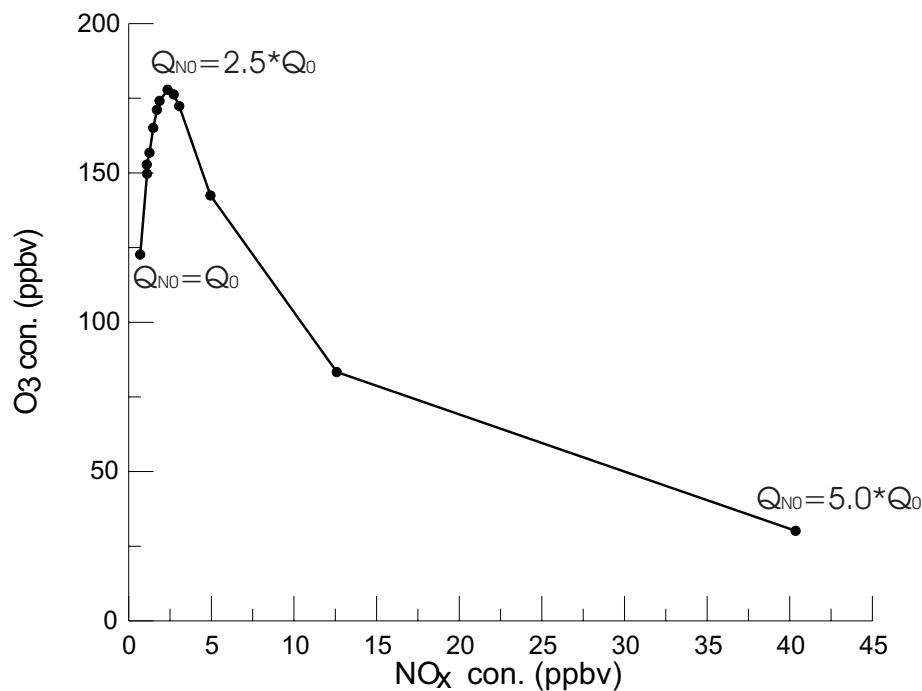


Fig. 6. O₃ vs. NO_x with different NO emission strengths after 5 days integration. The Q_{NO} is the NO emission strength; the Q_0 is the value in the PLUME case as given in Fig. 5.

[Title Page](#)[Abstract](#)[Introduction](#)[Conclusions](#)[References](#)[Tables](#)[Figures](#)[◀](#)[▶](#)[◀](#)[▶](#)[Back](#)[Close](#)[Full Screen / Esc](#)[Print Version](#)[Interactive Discussion](#)

**Numerical integration
of troposphere
photochemistry
mechanism**

F. Liu et al.

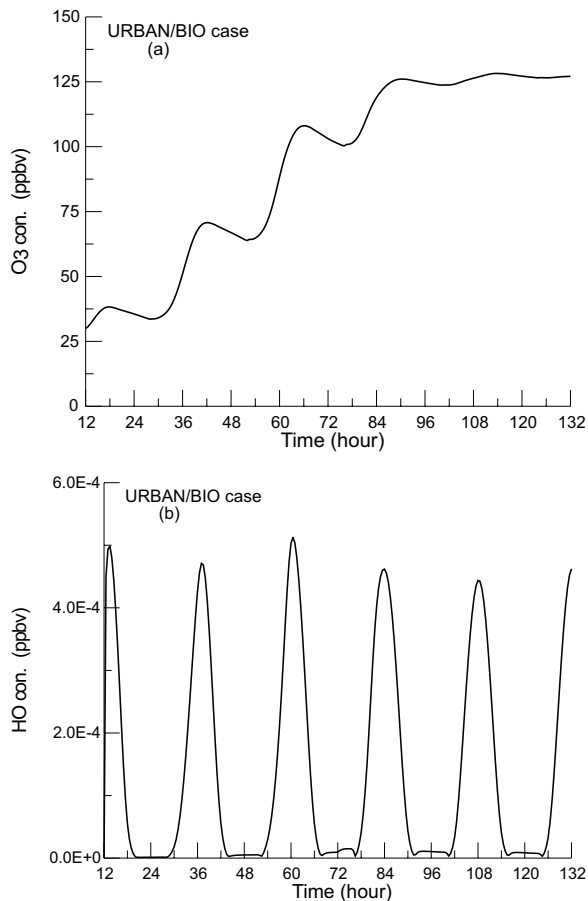


Fig. 7. The mixing ratio for O₃ (a), HO (b), NO (c), NO₂ (d), PAN (e), and RO₂ (f) as function of time for the URBAN/BIO case. The NO emission of $2.5 \cdot Q_0$ is switched off after 60 h and the biogenic emission of isoprene is switched on. The Q_0 is the value in the PLUME case as given in Fig. 5. The simulations start at noon with output every 30 min.

[Title Page](#)[Abstract](#)[Introduction](#)[Conclusions](#)[References](#)[Tables](#)[Figures](#)[◀](#)[▶](#)[◀](#)[▶](#)[Back](#)[Close](#)[Full Screen / Esc](#)[Print Version](#)[Interactive Discussion](#)

**Numerical integration
of troposphere
photochemistry
mechanism**

F. Liu et al.

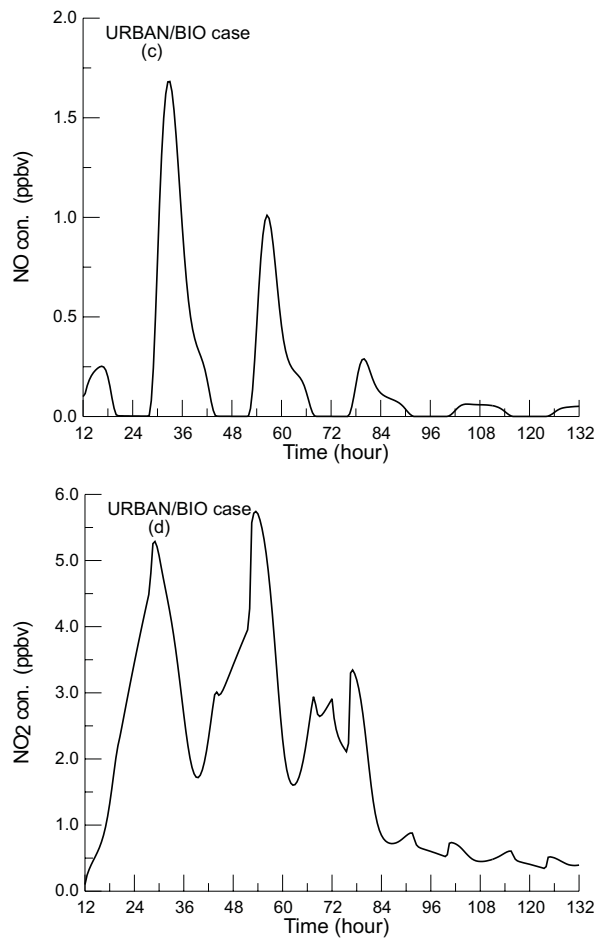


Fig. 7. Continued.

[Title Page](#)[Abstract](#)[Introduction](#)[Conclusions](#)[References](#)[Tables](#)[Figures](#)[◀](#)[▶](#)[◀](#)[▶](#)[Back](#)[Close](#)[Full Screen / Esc](#)[Print Version](#)[Interactive Discussion](#)

**Numerical integration
of troposphere
photochemistry
mechanism**

F. Liu et al.

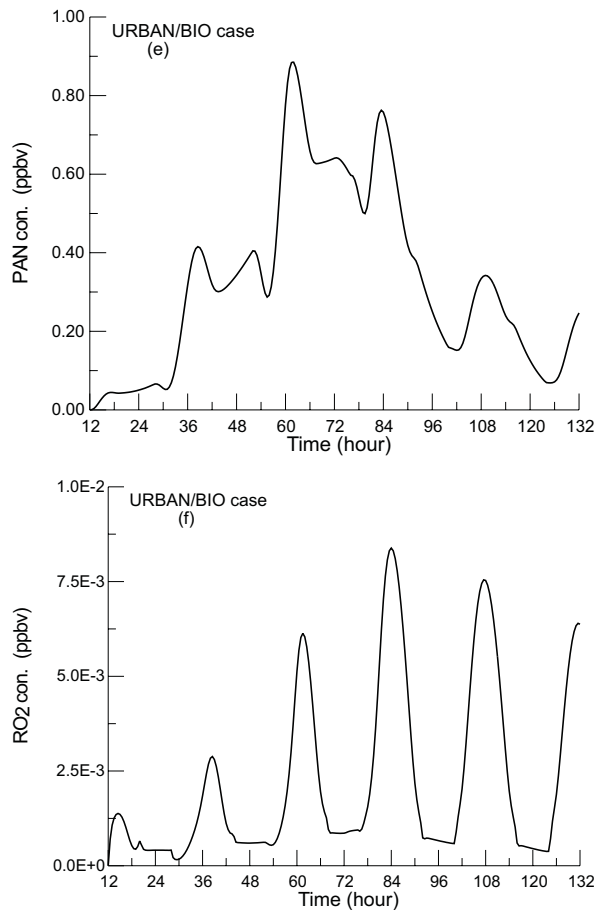


Fig. 7. Continued.

[Title Page](#)[Abstract](#)[Introduction](#)[Conclusions](#)[References](#)[Tables](#)[Figures](#)[◀](#)[▶](#)[◀](#)[▶](#)[Back](#)[Close](#)[Full Screen / Esc](#)[Print Version](#)[Interactive Discussion](#)

Numerical integration of troposphere photochemistry mechanism

F. Liu et al.

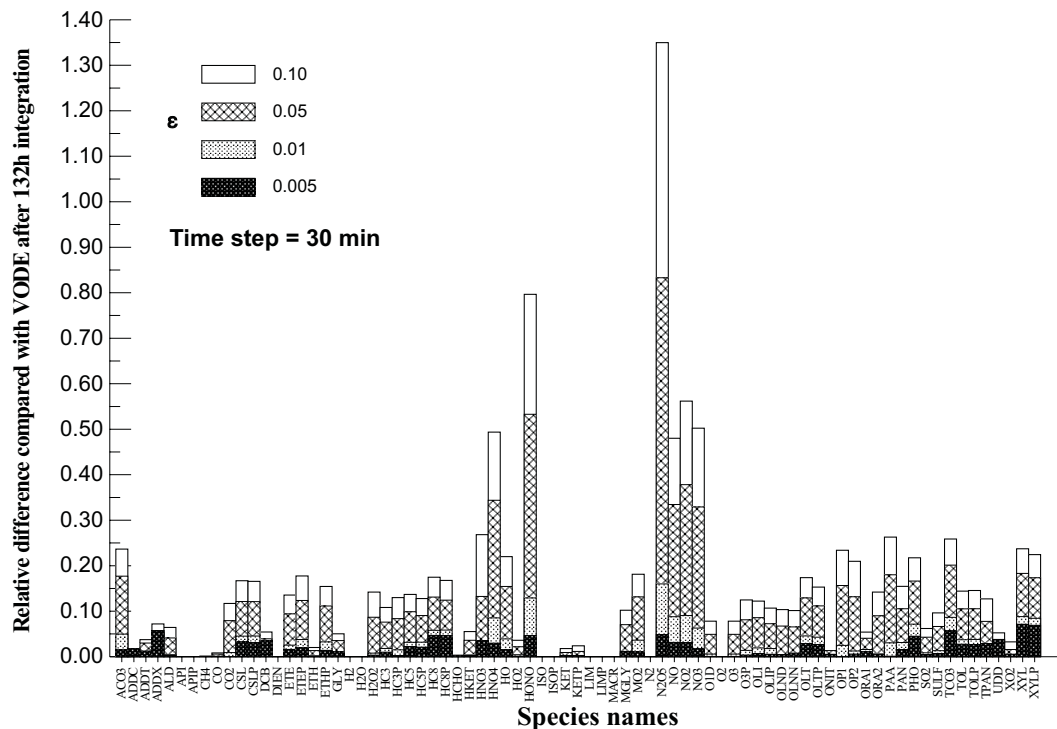


Fig. 8. The relative difference of mixing ratios compared with reference solutions for all species at end integration for the PLUME case. The calculated root mean square $e_{r.m.s}$ for the four accuracy levels ϵ 0.10, 0.05, 0.01 and 0.005 are 24.61%, 16.25%, 4.17% and 2.38%, respectively.

Title Page

Abstract

Introduction

Conclusions

References

Tables

Figures

⏪

⏩

◀

▶

Back

Close

Full Screen / Esc

Print Version

Interactive Discussion

Numerical integration
of troposphere
photochemistry
mechanism

F. Liu et al.

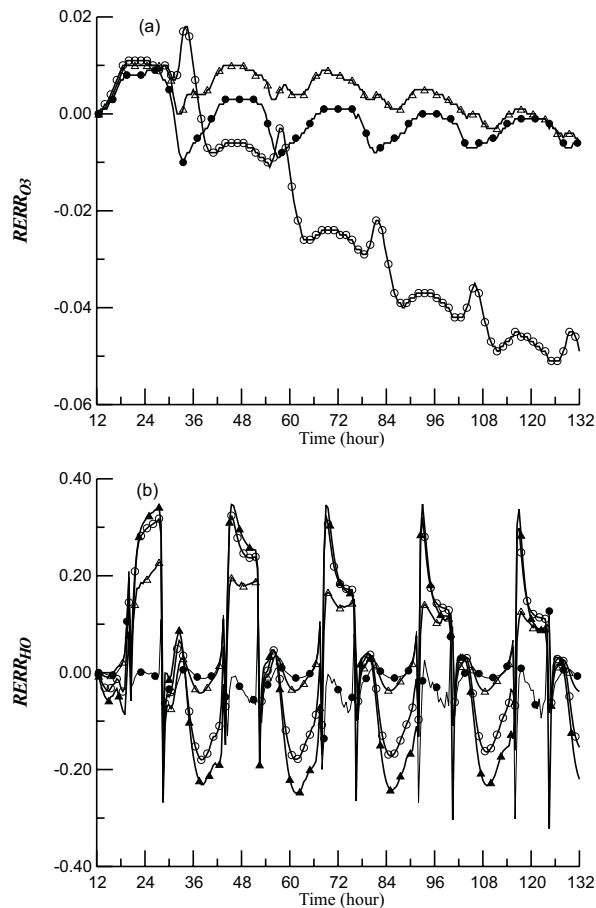


Fig. 9. The relative difference for O₃ (a), HO (b), NO (c), NO₂ (d), HONO (e), HCHO (f), PAN (g), and RO₂ (h) as function of time for the PLUME case. The simulations start at noon with output every 30 min (\blacktriangle : $\epsilon=0.10, Nc=1$; \circ : $\epsilon=0.05, Nc=1$; \triangle : $\epsilon=0.01, Nc=1$; \bullet : $\epsilon=0.005, Nc=5$).

Title Page

Abstract

Introduction

Conclusions

References

Tables

Figures

◀

▶

◀

▶

Back

Close

Full Screen / Esc

Print Version

Interactive Discussion

**Numerical integration
of troposphere
photochemistry
mechanism**

F. Liu et al.

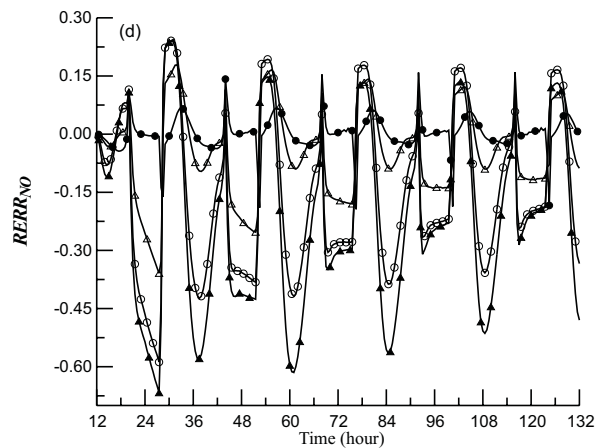
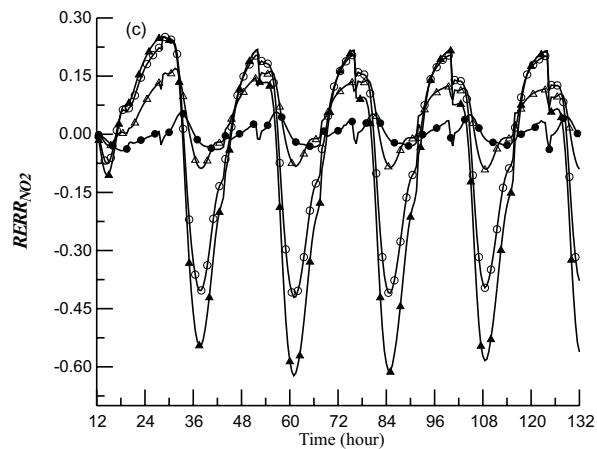


Fig. 9. Continued.

[Title Page](#)[Abstract](#)[Introduction](#)[Conclusions](#)[References](#)[Tables](#)[Figures](#)[◀](#)[▶](#)[◀](#)[▶](#)[Back](#)[Close](#)[Full Screen / Esc](#)[Print Version](#)[Interactive Discussion](#)

Numerical integration
of troposphere
photochemistry
mechanism

F. Liu et al.

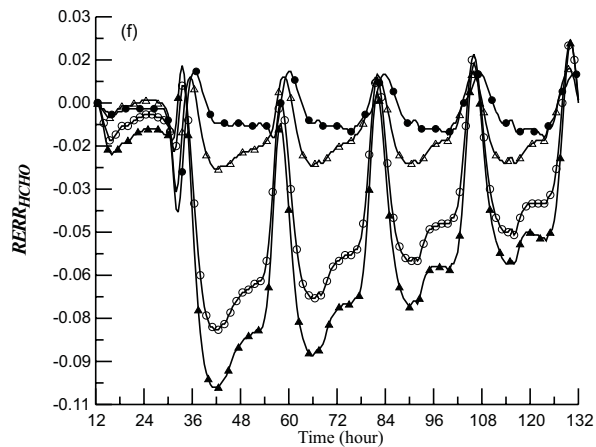
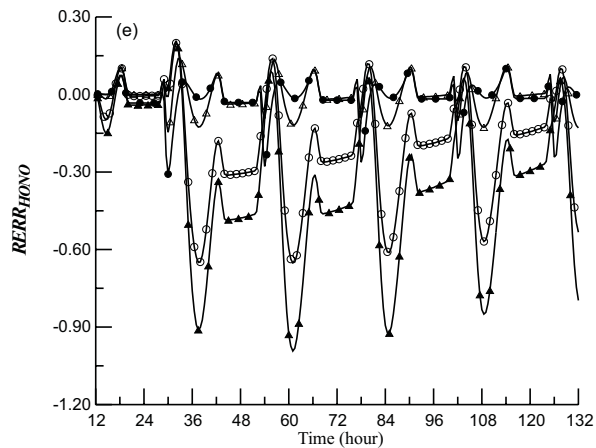


Fig. 9. Continued.

Title Page

Abstract

Introduction

Conclusions

References

Tables

Figures

◀

▶

◀

▶

Back

Close

Full Screen / Esc

Print Version

Interactive Discussion

Numerical integration
of troposphere
photochemistry
mechanism

F. Liu et al.

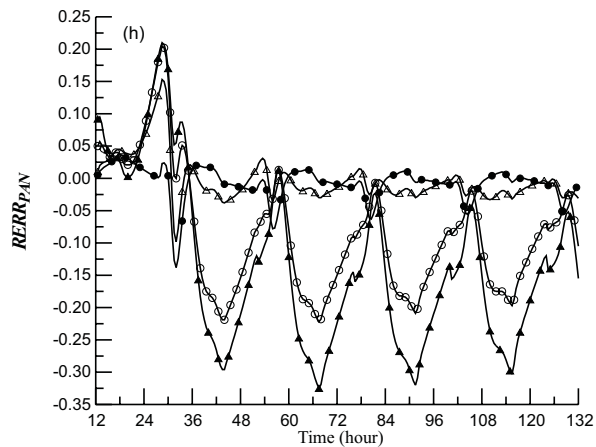
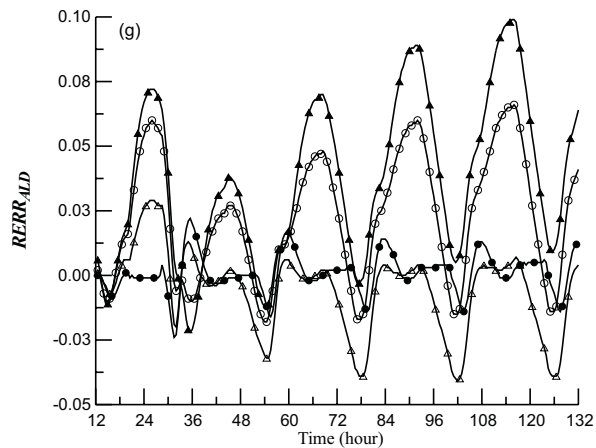


Fig. 9. Continued.

[Title Page](#)[Abstract](#)[Introduction](#)[Conclusions](#)[References](#)[Tables](#)[Figures](#)[◀](#)[▶](#)[◀](#)[▶](#)[Back](#)[Close](#)[Full Screen / Esc](#)[Print Version](#)[Interactive Discussion](#)

Numerical integration of troposphere photochemistry mechanism

F. Liu et al.

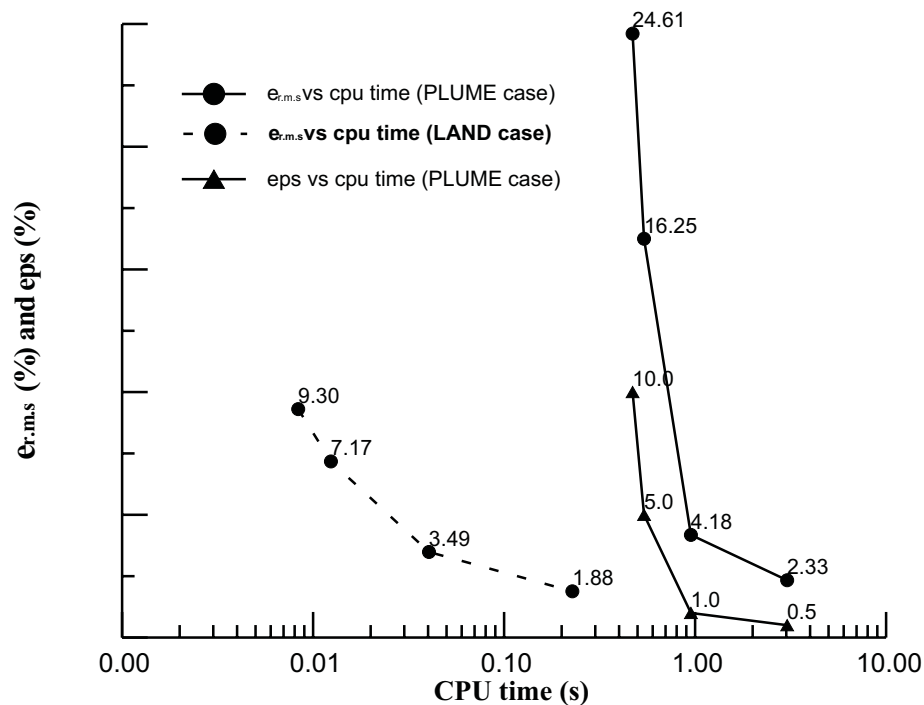


Fig. 10. Accuracy vs. CPU time. The $e_{r.m.s}$ is root mean square of relative difference for all species in the RACM. The eps (%) stands for predictor-corrector error tolerance ε in the CHEMEQ2. (Solid line: the PLUME case and dashed line: the LAND case).

Title Page

Abstract

Introduction

Conclusions

References

Tables

Figures

◀

▶

◀

▶

Back

Close

Full Screen / Esc

Print Version

Interactive Discussion

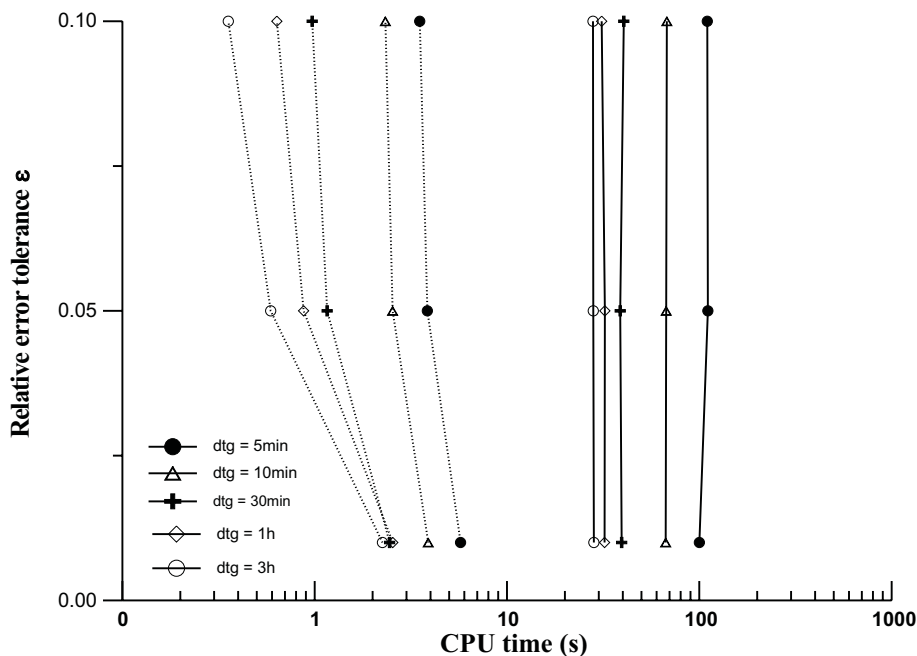


Fig. 11. Comparison of CPU time used by VODE and CHEMEQ2 solvers for 5 days simulations. The simulations are implemented with five scales of global time step ($\Delta t_g = 5$ min, 10 min, 30 min, 1 h and 3 h) and three accuracy levels ($\varepsilon = 0.10, 0.05, 0.01$). (Solid line: VODE, dashed line: CHEMEQ2).

Numerical integration of troposphere photochemistry mechanism

F. Liu et al.

Title Page

Abstract

Introduction

Conclusions

References

Tables

Figures

◀

▶

◀

▶

Back

Close

Full Screen / Esc

Print Version

Interactive Discussion

EGU

**Numerical integration
of troposphere
photochemistry
mechanism**F. Liu et al.

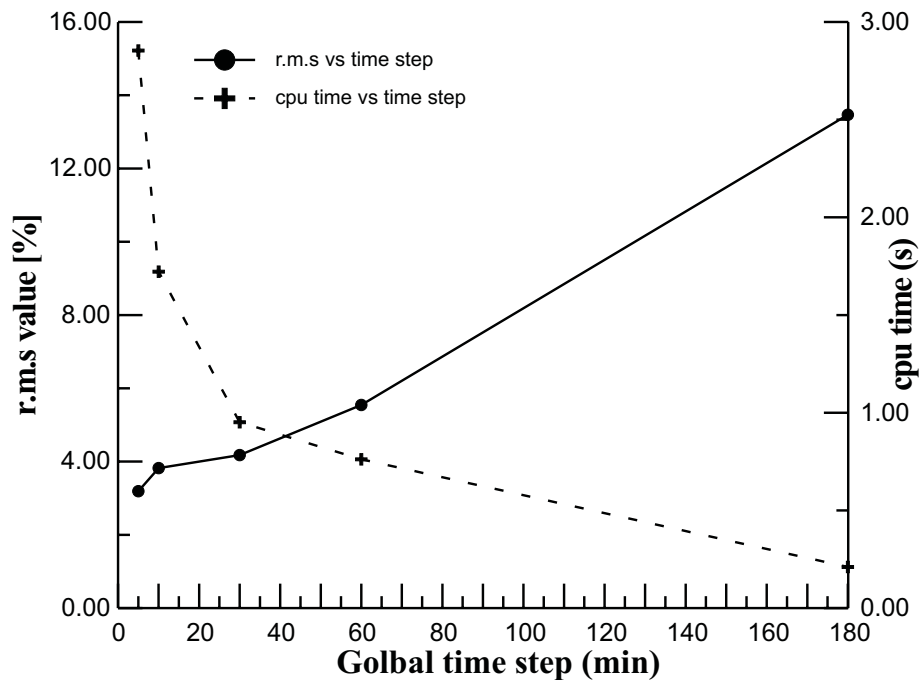


Fig. 12. The variations of *r.m.s* of relative difference and CPU time against global time step Δt_g .

[Title Page](#)[Abstract](#)[Introduction](#)[Conclusions](#)[References](#)[Tables](#)[Figures](#)[◀](#)[▶](#)[◀](#)[▶](#)[Back](#)[Close](#)[Full Screen / Esc](#)[Print Version](#)[Interactive Discussion](#)